Preferential Interactions of Glycine Betaine and of Urea with DNA: Implications for DNA Hydration and for Effects of These Solutes on DNA Stability[†]

Jiang Hong,[§] Michael W. Capp,[‡] Charles F. Anderson,[‡] Ruth M. Saecker,[‡] Daniel J. Felitsky,[§] Melissa W. Anderson,[||] and M. Thomas Record,Jr.*[,§,‡]

Department of Biochemistry, Department of Chemistry, and Program in Biophysics, University of Wisconsin-Madison, Madison, Wisconsin 53706

Received May 4, 2004; Revised Manuscript Received August 6, 2004

ABSTRACT: Interactions of the solutes glycine betaine (GB) and urea with mononucleosomal calf thymus DNA in aqueous salt solutions are characterized by vapor pressure osmometry (VPO). Analysis of osmolality as a function of solute and DNA concentration yields the effect of the solute on the chemical potential, μ_2, of the DNA. Although both GB and urea generally are nucleic acid denaturants and therefore must interact favorably with the nucleic acid surface exposed upon melting, VPO demonstrates that neither interacts favorably with duplex DNA. Addition of GB greatly increases μ_2 of DNA, indicating that the average local concentration of GB in the vicinity of the double helix is much less than its bulk concentration. By contrast, addition of urea has almost no effect on μ_2 of duplex DNA, indicating that the average local concentration of urea in the vicinity of duplex DNA is almost the same as in bulk solution. Qualitatively, we conclude that the nonuniform distribution of GB occurs primarily because duplex DNA and GB prefer to interact with water rather than with each other. Comparison with thermodynamic data for the interaction of GB with various protein surfaces (Felitsky et al., *Biochemistry*, *43*, 14732−14743) shows that GB is excluded primarily from anionic DNA surface and that the hydration of anionic DNA phosphate oxygen surface ($\gtrsim$17 H_2O per nucleotide or $\gtrsim$0.22 H_2O Å^{-2}) involves at least two layers of water. From analysis of literature data for effects of urea and of GB on DNA melting, we propose that urea is an effective nonspecific nucleic acid denaturant because of its favorable interactions with the polar amide-like surface of G, C, and especially T or U bases exposed in denaturation, whereas GB is a specific GC denaturant because of its favorable interaction with G and/or C surface in the single-stranded state.

Glycine betaine (GB)[1] and urea exhibit very different effects on protein folding and other protein processes and interact very differently with folded and unfolded protein surfaces (*1*−*4*). In our research, we have focused on this pair of solutes to understand the molecular and thermodynamic basis of both osmoprotection and the effect of these solutes on biopolymer processes (*1*−*4*). Toward these goals, it is important to quantify the interaction of GB and of urea with double- and single-stranded nucleic acid surfaces. At molar concentrations, both solutes destabilize the double-helical conformation of naturally occurring nucleic acids; thermal transition temperatures, T_m, decrease approximately linearly with increasing solute concentration (*5*−*9*). This dependence indicates that both solutes must interact favorably with, and therefore accumulate at, the uncharged nucleic acid surface exposed in the conformational transition to the single-stranded state. Von Hippel and co-workers (*5*) observed that the destabilizing effect of GB on DNA increases with increasing fraction of GC base pairs; thermal stability of poly(dAT) is almost unaffected (possibly slightly increased) by addition of GB. By contrast, the effect of urea on T_m of DNA is not a function of base composition (*6*).

Quantitative thermodynamic information regarding the interactions of various solutes with native protein surface has been obtained by dialysis in conjunction with densimetry (*10*, *11*), by ultracentrifugation (*12*, *13*), and by vapor pressure osmometry (VPO; *2*, *4*, *14*). In particular, interactions of GB and of urea with native protein surface have been quantified by VPO (*2*, *4*). Additionally, interactions of GB and of urea with the surface exposed in unfolding the marginally stable lacI HTH DNA binding domain and other proteins and peptides have been characterized by quantitative studies of unfolding (*1*, *15*, *16*). Results of these studies have been analyzed using the solute partitioning model (local−bulk domain model) and calculated water-accessible surface areas (ASA) (*1*−*4*, *17*, *18*). We find that urea interacts favorably with (i.e., accumulates at) both folded protein surface and the surface exposed in unfolding proteins and α-helical peptides. Quantitative comparisons of the extent

[†] Support of this research by NIH Grants GM 47022 and GM 23467 is gratefully acknowledged.

* To whom correspondence should be addressed. Mailing address: Department of Biochemistry, 433 Babcock Drive, University of Wisconsin-Madison, Madison, WI 53706. Tel: (608) 262−5332. Fax: (608) 262−3453. E-mail: record@biochem.wisc.edu.

[§] Department of Biochemistry.

[‡] Department of Chemistry.

[||] Program in Biophysics.

[1] Abbreviations: VPO, vapor pressure osmometry; ASA, water-accessible surface area; GB, glycine betaine (*N*,*N*,*N*-trimethyl glycine); lacI, lac repressor; HTH, helix-turn-helix domain; BSA, bovine serum albumin; HEWL, hen egg white lysozyme.

10.1021/bi049096q CCC: $27.50
Published on Web 10/30/2004

Table 1: Surface Area (ASA) Composition of DNA and of Protein or Peptide

	total ASA (Å^2)	charged ASA (Å^2)[a]	polar amide ASA (Å^2)[a]	other polar ASA (Å^2)[a]	nonpolar ASA (Å^2)[a]
ds DNA (50% GC)[b]	171	negative, 74 (44%)	4.2 (2.5%)	27 (16%)	65 (38%)
ss DNA (half stacked, 50% GC)[b]	269	negative, 67 (25%)	40 (15%)	70 (26%)	92 (34%)
ASA$^\Delta$ for ds → ss (half stacked, 50% GC)[b]	98	negative, −7 (−7%)	36 (37%)	43 (44%)	26 (26%)
native BSA[c]	2.78×10^4	negative, 16% positive, 13%	15%	3%	53%
native HEWL[c]	6.5×10^3	negative, 4.5% positive, 17%			
ASA$^\Delta$ for lacI HTH unfolding[c]	3.5×10^3	negative, 2.2% positive, 4.1%	16%	5.2%	72%
ASA$^\Delta$ for unfolding alanine-based α-helical peptides		2.5%	57%	0	40%

[a] Definitions of negatively charged ASA, polar amide-like and other polar ASA, and nonpolar ASA of DNA are given in text. [b] Values are expressed per nuclotide. [c] From Felitsky et al. (*66*).

of interaction of urea with these different protein surfaces led to the proposal that urea is accumulated only at polar amide/peptide surface (*4*); here we test the generality of this proposal by quantifying interactions of urea with duplex DNA and with the surface exposed in DNA melting, which includes amide-like functional groups on C, G, and especially T (but not A) bases. (Henceforth, for ease of reference, the term "polar amide surface" defined in Methods will be applied to both proteins and nucleic acids.)

GB, in contrast to urea, interacts unfavorably with (i.e., is excluded from) all protein surfaces examined. These protein surfaces prefer to interact with water rather than with GB. Local/bulk GB concentration ratios (partition coefficients) obtained from the solute partitioning model are less than unity for all protein surfaces, being smallest for folded bovine serum albumin (BSA) surface, larger for folded HEWL (hen egg white lysozyme) surface, and largest for the surface exposed in unfolding the lacI HTH and other globular proteins. As discussed elsewhere (*66*), this pattern of interactions correlates principally with the fraction of water-accessible anionic (carboxylate) oxygen surface and leads to the proposal that the strongly favorable interactions of carboxylate oxygen surface with water cause GB to be completely excluded from the water of hydration of protein anionic oxygens. Previously, no quantitative information has been reported for interactions of either GB or urea with DNA surface.

In the present study, we report an extensive series of osmometric (VPO) data that characterize the interactions of GB and of urea with native calf thymus (mononucleosomal) DNA at ∼0.2 and ∼0.4 *m* univalent salt concentration. Native DNA surface is dominated by anionic (phosphate) oxygens (44%, cf. Table 1), allowing us to predict strong exclusion of GB from native DNA surface. Accumulation of urea in the vicinity of both folded and unfolded protein surface exhibits little if any correlation with the fraction of charged surface. Urea is neither accumulated nor excluded from the vicinity of salt ions (K^+, Na^+, Cl^-) in solution (*19*). Native DNA surface is almost devoid of carbonyl oxygens or other amide-like functional groups (∼2%). On this basis, urea is predicted to exhibit no strong preferential interaction with native DNA. The experimental results reported herein are consistent with these predictions based on protein and model compound data. Effects of GB and of urea on DNA stability are interpreted quantitatively in terms of interactions of these solutes with the DNA surface exposed in melting and compared with their interactions with native DNA surface. We deduce that urea is an effective nonspecific nucleic acid denaturant because of its favorable interactions with the polar amide surface areas (defined in Methods) of G, C, and especially T bases exposed in denaturation, whereas GB is a specific GC denaturant because of its favorable interaction with G or C surface or both in the single-stranded state.

BACKGROUND

Quantifying Solute−Biopolymer Interactions and Their Effects on Biopolymer Processes. Biopolymer processes are affected by a spectrum of solutes including denaturants (e.g., urea, GuHCl), osmolytes (e.g., GB), and electrolytes (e.g., Hofmeister salts), which generally do not bind stoichiometrically to individual sites on any biopolymer involved in the process (see ref *18* for a review). Concentration-dependent effects of solutes on biopolymer processes (e.g., conformational changes, ligand binding) result in general from the preferential interactions of these solutes with biopolymers (local accumulation or exclusion relative to their bulk concentration) that change the activity coefficients of product and reactant biopolymers to different extents.

Under typical experimental conditions, where a nonelectrolyte solute (3) is in substantial excess over all stoichiometric participants of a biopolymer process, the effect of its activity (a_3) on the "phenomenological" equilibrium concentration quotient (K_{obs}) for any biopolymer process is related to the relevant individual values of thermodynamic functions, Γ_{μ_3}, usually called preferential interaction coefficients (*20*):

$$\left(\frac{\partial \ln K_{obs}}{\partial \ln a_3}\right)_{T,P} = \Delta\Gamma_{\mu_3} \quad (1)$$

where $\Delta\Gamma_{\mu_3}$ is the stoichiometrically weighted difference between values of Γ_{μ_3} characteristic of interactions of the solute (3) with each product and reactant (component 2) in the process. For the situation in which only one small solute (component 3) is present, typically in excess of the biopolymer (component 2), each Γ_{μ_3} is fundamentally defined as the change in molal concentration of the small solute (m_3) required to keep its chemical potential (μ_3) constant when the concentration of the biopolymer (m_2) changes. These

coefficients also describe the effect of changing a_3 on the molal-scale activity coefficient, γ_2, of the biopolymer:

$$\Gamma_{\mu_3} \equiv \left(\frac{\partial m_3}{\partial m_2}\right)_{T,P,\mu_3} = -\frac{\mu_{32}}{\mu_{33}} = -\frac{\mu_{23}}{\mu_{33}} = -\left(\frac{\partial \ln \gamma_2}{\partial \ln a_3}\right)_{T,P,m_2} \quad (2)$$

where the chemical potential derivatives μ_{ij} are defined as $\mu_{ij} \equiv (\partial\mu_i/\partial m_j)_{T,P,m_{j'\neq j}}$ where $i, j = 2$ or 3. (The equality of μ_{32} and μ_{23} follows from Euler reciprocity of cross-partial derivatives.) Positive values of $\Delta\Gamma_{\mu_3}$ imply that solute (3) exhibits more favorable (or less unfavorable) preferential interactions with products than with reactants so that, according to eq 2, increasing the concentration (hence activity) of the small solute increases K_{obs}. Values of $\Delta\Gamma_{\mu_3}$ for a process are interpreted as the preferential interaction of the solute with the biopolymer surface that is exposed to solvent (or buried from solvent) in the process (*3*). Interpretations of $\Delta\Gamma_{\mu_3}$ for effects of urea or GB on protein−DNA interactions require independent information about the interactions of each of these solutes with DNA and with protein surface. Generalization of eqs 1 and 2 to systems in which two small solutes are present in excess is required to analyze (for example) protein−nucleic acid binding as a function of urea or GB concentration in a solution that also contains salt (Hong et al., manuscript in preparation). The relevant (four-component) preferential interaction coefficient (the extension of eq 2 to a four-component system) required to analyze the preferential interaction of GB or urea with DNA in a salt solution is given in the section on data analysis.

Quantifying μ_{23} and Γ_{μ_3} by Vapor Pressure Osmometry (VPO). By definition, osmolality, directly measurable (for example) with a water vapor pressure osmometer, is related to the activity of solvent water, $a_1 = \gamma_1 x_1$ (where x_1 is the mole fraction of water and γ_1 the corresponding activity coefficient) by

$$\text{Osm} \equiv -m_1^\bullet \ln a_1 \quad (3)$$

where $m_1^\bullet \equiv 55.5$ mol kg^{-1}, the constant "molality" of pure water. In an ideal dilute solution of one nonelectrolyte solute, as its mole fraction approaches zero, the osmolality is equal to the solute molality; osmolality deviates from molality with increasing molality as a consequence of water−solute interactions, binding of water to the solute, or both. Similarly, the osmolality of a three-component solution (Osm(m_2,m_3)) generally differs from the sum of the osmolalities of the two corresponding two-component solutions (Osm(m_2), Osm(m_3)). This difference is defined as Δ_{23}Osm:

$$\Delta_{23}\text{Osm} \equiv \text{Osm}(m_2,m_3) - \text{Osm}(m_2) - \text{Osm}(m_3) \quad (4)$$

Robinson and Stokes (*21*) proposed a remarkably simple approximate relationship linking Δ_{23}Osm to the chemical potential derivative μ_{23} (introduced in eq 2):

$$\mu_{23} \cong \frac{RT\Delta_{23}\text{Osm}}{m_2 m_3} \quad (5)$$

Hence, Δ_{23}Osm provides an experimental route to Γ_{μ_3} via μ_{23} as demonstrated by ref *19*. In all other previous applications of eq 5 to isopiestic distillation (ID) data (e.g., refs *21* and *22*), the objective was to quantify, via integration of μ_{23}, the activity coefficients of solutes 2 and 3 as functions of their molalities. Extension of eqs 2−5 to four-component (water, DNA, solute, salt) solutions are given in Methods of Analysis. The approximations underlying eq 5, which are justified for the solute concentrations investigated here, are analyzed elsewhere (Anderson et al., manuscript in preparation).

METHODS

Experimental Procedures

Mononucleosomal Calf Thymus DNA. DNA of 160 ± 5 bp length was prepared as described by Wang et al. (*23*). Solutions at DNA concentrations of ∼0.2 *m* in nucleotide monomer were extensively dialyzed at 4 °C, first against a solution containing 10 mM HEPES buffer at pH 6.5, together with 100 mM KCl (or NaCl) and 2 mM EDTA, then against 10 mM KCl (or NaCl), and finally twice against 2.5 mM KCl (or NaCl). Prepared by this method, DNA is monodisperse and double-helical (*23*, *24*). After each sequence of dialyses, the DNA solutions were concentrated by speed vacuum concentrator, and ultrapure deionized water was added, if necessary, to produce a final DNA phosphate concentration in the range 0.3−0.4 *m*. Higher DNA concentrations are too viscous to transfer with quantitative accuracy, limiting the maximum DNA phosphate concentration for osmometry to 0.2 *m*. NaDNA samples prepared in this manner contain a small (0−10%) residual amount of salt (presumably NaCl) per DNA phosphate (*25*). Donnan membrane equilibrium calculations for the conditions of our dialysis experiments on Na (or K) DNA solutions, using the limiting value of Donnan equilibrium coefficient (−0.06 (*26*−*28*)), indicate a concentration of residual salt of ∼5% of the DNA phosphate molality; using the limiting osmotic coefficient (0.12 (*29*)) for DNA solution and assuming additivity to interpret the experimental (VPO) osmolalities of DNA stock solution indicates a concentration of residual salt of ∼10% of the DNA phosphate molality. Systematic use of either one of these amounts (or zero) residual KCl (or NaCl) has no significant affect on the calculation of either the chemical potential derivatives or the preferential interaction coefficients reported here.

Solutes. Glycine betaine monohydrate (>99% pure, FW 135.16) was obtained from Sigma (St. Louis, MO), and urea was obtained from Fluka Biochemika and Life Technologies, as described previously (*19*). NaCl (certified ACS, FW 58.44, 99.5% pure) was obtained from Fisher Scientific. KCl (FW 74.56) was obtained from Aldrich (99.999% pure) and from Fisher Scientific (certified ACS, 99.5% pure); the two sources of KCl exhibited identical VPO measurements under the same solution conditions.

Preparation of Samples for VPO. For each sequence of VPO measurements (e.g., Osm(m_2,m_3,m_4) vs m_3 at constant m_2 and m_4 or Osm(m_3,m_4) vs m_3 at constant m_4), concentrated stock solutions of urea (0.25−7 *m*) or GB (0.05−4 *m*), KCl or NaCl (2−4 *m*), and KDNA or NaDNA were carefully prepared using gravimetric methods whenever possible. For all stock solutions, densities were measured with a vibrating-tube density meter (DMA 5000, Anton Paar) to calculate the final concentrations of all components in VPO samples or to calculate the amount of the stock needed in preparing each VPO sample. (Densities of DNA stock solutions were

measured for representative samples.) Predetermined amounts of the stock solutions were combined gravimetrically. For these VPO sample preparations, the requisite amounts of stock solutions were determined according to the following considerations: maintaining the molality of DNA and salt constant across the solute titration series, varying urea or GB molality (m_3) over a range sufficient to provide an adequate distribution of data points, ensuring enough volume for triplicate readings of each VPO sample, and maintaining the total solute molalities within levels such that the osmolality does not exceed the operating range of the osmometer ($\lesssim$3.5 Osm). Concentrations of DNA stock solutions were determined after gravimetric serial dilutions from the UV absorbance at 260 nm using the extinction coefficient $\epsilon = 0.0185$ (μg/mL)$^{-1}$ cm^{-1} for KDNA and $\epsilon = 0.0195$ (μg/mL)$^{-1}$ cm^{-1} for NaDNA, both of which were calculated using formulae 6−10 in Bloomfield et al. (*30*).

Whenever volumetric steps (with pipetted volume calibrated gravimetrically) were used (in our early data sets), apparent partial molar volumes were used in calculating sample molalities (cf. eqs 15 and 16 of ref *2*). No significant differences between volumetric and gravimetric data were observed for our DNA solutions in the concentration range investigated, in contrast to the situation observed for concentrated BSA solutions (*66*). Apparent partial molar volumes in corresponding two-component solutions determined in this study (or taken from the literature, as noted) are as follows: 0.1744 L/mol for monomer NaDNA, which is constant within the experimental concentration range (from 0.06 to 0.24 M in phosphate monomer) and which is within the broad range of literature values (*31*−*33*); 0.1855 L/mol for monomer KDNA, in good agreement with the literature value for *Escherichia coli* bacteriophage T4 KDNA (*34*); 0.017 45 + 0.001 119m_{NaCl} L/mol for NaCl and 0.027 57 + 0.001 301m_{KCl} L/mol for KCl, which agree well with literature values (*35* and references given there) over the concentration range investigated in our VPO study (0.2−0.8 *m* salt); 0.0982 ± 0.0003 L/mol for GB (*2*, *36*); 0.044 23 L/mol for urea (*3*, *37*, *38*). The difference in apparent partial molar volumes between KDNA and NaDNA is approximately the same as that between KCl and NaCl. The effect of a small potential systematic error (~6%) in the apparent molar volumes of DNA on the calculated values of preferential interaction coefficients was examined and found to be negligible (~0.1%). For VPO experiments, the molality (m_4) of KCl (or NaCl) is fixed at approximately 0.2 or 0.4 *m*, and (when present) the molality of DNA phosphate (m_{2u}) is fixed at approximately 0.1 or 0.2 *m*. Salt and DNA concentrations in these four-component solutions are known to ±3% and ±2%, respectively. For each titration with urea or GB, m_3 varies over the range from 0.1 to 2.3 *m* (for urea) or to 1.35 *m* (for GB).

VPO Determination of Osmolality as a Function of Small Solute Concentration. Background on the theory and practice of VPO relevant to the present study has been provided previously (*2*, *14*, *19*). Two osmometers, Wescor 5500 at working temperature 37 °C and VAPRO 5520 (Logan, UT) at (controlled) ambient temperature (~25 °C), were used for measurements on different series of samples; no significant differences between results obtained from the two osmometers were found for VPO measurements under the solution conditions in this study. All osmolalities were corrected to account for minor discrepancies between currently accepted literature values and those assigned to the standard solutions containing specified molalities of NaCl (as provided by Wescor) (*19*).

Among all data sets for GB and urea, 13 four-component and 18 three-component data sets were collected at constant molality of DNA and of salt. Our early VPO experiments on GB (four data sets for four-component and two for three-component systems) were performed by holding the molarity of DNA, the salt or both constant, for which the ratio of molalities m_{2u}/m_4 was constant, but m_{2u} and m_4 increased systematically by up to 12% with increasing m_3 in the ranges investigated. To analyze these constant molarity data, conversions from constant molarity to constant molality constraints on the calculated derivatives were performed (as explained in the section on VPO Data Analysis).

Methods of Analysis

Four-Component Preferential Interaction Coefficients, Γ_{μ_3,m_4} Characterizing Solute−DNA Interactions in Salt Solutions. For a series of four-component solutions, such as aqueous solutions of DNA (component 2) containing variable concentrations of a small solute (component 3; urea or GB) and a fixed concentration of salt (component 4; KCl or NaCl), the analogue of eq 2 is

$$\Gamma_{\mu_3,m_4} \equiv \left(\frac{\partial m_3}{\partial m_2}\right)_{T,P,\mu_3,m_4} = -\frac{\mu_{32,4}}{\mu_{33,4}} = -\frac{\mu_{23,4}}{\mu_{33,4}} = -\left(\frac{\partial \ln \gamma_2}{\partial \ln a_3}\right)_{T,P,m_2,m_4} \quad (6)$$

where the chemical potential derivatives $\mu_{ij,4}$ are defined as $(\partial\mu_i/\partial m_j)_{T,P,m_{j'\neq j},m_4}$ for $i = 1$, 2, or 3 and $j = 2$ or 3. The equality of $\mu_{32,4}$ and $\mu_{23,4}$ follows from Euler reciprocity of cross-partial derivatives.

Quantifying $\mu_{23,4}$ and Γ_{μ_3,m_4} by Vapor Pressure Osmometry (VPO). In our investigation of interactions of a nonelectrolyte solute (component 3; urea or GB) with DNA, a fourth component (NaCl or KCl) also is present at constant molality. In this situation (i.e., where Osm(m_2) and Osm(m_2,m_3) are experimentally inaccessible), $\Delta_{23,4}$Osm, the four-component analogue of eq 4, is the difference between the effect on osmolality when solute 3 is added to a solution containing solutes 2 and 4 (Osm (m_2,m_3,m_4) − Osm(m_2,m_4)) and its effect on osmolality when added to a solution containing only solute 4 ((Osm(m_3,m_4) − Osm(m_4)):

$$\Delta_{23,4}\text{Osm} \equiv (\text{Osm}(m_2,m_3,m_4) - \text{Osm}(m_2,m_4)) - (\text{Osm}(m_3,m_4) - \text{Osm}(m_4)) \quad (7)$$

This difference of differences ($\Delta_{23,4}$Osm) is approximately related to $\mu_{23,4}$ by the analogue of eq 5:

$$\mu_{23,4} \cong \frac{RT\Delta_{23,4}\text{Osm}}{m_2 m_3} \quad (8)$$

Equation 8 for a four-component system is expected to be accurate if the presence of DNA does not affect the dependence of the chemical potential of solute (3) on the molality of salt (4), so that the derivative μ_{34} is the same in the presence or absence of component 2 ($\mu_{34}(m_2,m_3,m_4) \approx$

$\mu_{34}(m_3,m_4)$) (Anderson et al., manuscript in preparation). The preferential interaction coefficient Γ_{μ_3,m_4} characterizing solute−DNA interaction at fixed salt concentration is evaluated from $\mu_{23,4}$ (eq 8) using the third equality in eq 6 ($\Gamma_{\mu_3,m_4} = -\mu_{23,4}/\mu_{33,4}$). In this expression for Γ_{μ_3,m_4}, the quantity $\mu_{33,4}$ is related to $\mu_{23,4}$ and other chemical potential derivatives by the Gibbs−Duhem equation:

$$m_3\mu_{33,4} = -m_1\mu_{13,4} - m_2\mu_{23,4} - m_4\mu_{43,4} \qquad (9A)$$

In eq 9A, $\mu_{13,4}$ is obtained by analysis of the osmolality data for the four-component solution as a function of m_3:

$$-m_1\mu_{13,4} = RT\left(\frac{\partial \mathrm{Osm}(m_2,m_3,m_4)}{\partial m_3}\right)_{T,P,m_2,m_4} \qquad (10)$$

The chemical potential derivative $\mu_{43,4} \equiv \mu_{43}(m_2,m_3,m_4)$ in eq 9A is approximated by its counterpart $\mu_{43}(m_3,m_4)$ in the corresponding three-component system, which is obtained from VPO (see Appendix A). As an adequate alternative to eq 9A, $\mu_{33,4}$ may be approximated by the two-component derivative, $\mu_{33}(m_3)$:

$$\mu_{33,4} \cong \mu_{33}(m_3) = (RT/m_3)\left(\frac{\partial \mathrm{Osm}(m_3)}{\partial m_3}\right)_{T,P} \qquad (9B)$$

Within the uncertainty of the experimental data, these alternative methods of determining $\mu_{33,4}$ (eqs 9A and 9B) are found to yield the same result for Γ_{μ_3,m_4} describing interactions of GB or urea with native DNA under the conditions investigated here.

Preferential Interaction Coefficient Expressed per DNA Nucleotide Monomer. The molality of the DNA is conventionally expressed per monomer unit: $m_{2u} \equiv N_u m_2$, where N_u is the average number of monomer units (nucleotides) per DNA molecule ($N_u = 320$ for mononucleosomal calf thymus DNA). Accordingly, the values of Γ_{μ_3,m_4} and $\mu_{23,4}$ are reported here on a DNA monomer basis:

$$\mu_{2u3,4} \equiv \mu_{23,4}/N_u; \quad \Gamma^u_{\mu_3,m_4} \equiv \Gamma_{\mu_3,m_4}/N_u = -\mu_{2u3,4}/\mu_{33,4} \qquad (11)$$

For the local−bulk solute partitioning anslysis (see eq 13) of preferential interaction coefficients, the dependence of $\Gamma^u_{\mu_3,m_4}$ on the bulk concentration of solute (m_3^{bulk}) is required. Once $\Gamma^u_{\mu_3,m_4}$ is known, m_3^{bulk} is calculated from m_3 using the relationship (*2*)

$$m_3^{bulk} \cong m_3 - m_{2u}\Gamma^u_{\mu_3,m_4} \qquad (12)$$

For GB and urea at the DNA concentrations investigated, m_3^{bulk} differs from m_3 by ≤6%.

VPO Data Analysis. Calculations of $\Delta_{23,4}$Osm using eq 7 were performed for each Osm(m_2,m_3,m_4) obtained by averaging triplicate VPO readings on an individual sample. These values of Osm(m_2,m_3,m_4) at constant m_2 and m_4 and variable m_3 were also fitted as described below and extrapolated to $m_3 = 0$ to obtain the appropriate Osm(m_2,m_4) as input for eq 7 for $\Delta_{23,4}$Osm. Determinations of Osm(m_3,m_4) at the same fixed m_4 as used in the measurement of Osm(m_2,m_3,m_4) and variable m_3 were fitted and interpolated to the corresponding m_3 for each four-component experiment; extrapolation of Osm(m_3,m_4) to $m_3 = 0$ provided the appropriate Osm(m_4) for analysis of $\Delta_{23,4}$Osm (using eqs 7 and 8). Extrapolation to obtain the appropriate Osm(m_2,m_4) and Osm(m_4) is preferable to direct measurement because of small (typically ≤0.5%) variations in m_{2u}, m_4, or both for the independently prepared samples that make up a VPO series. Differences between extrapolated values and those directly measured by VPO (Osm(m_2,m_4)) or calculated (Osm(m_4)) using literature formulas (*39*, *40*) are typically less than ∼0.7%. Use of extrapolated values of Osm(m_2,m_4) and Osm(m_4) reduces the uncertainty (scatter) in the analysis of very weak interactions (e.g., urea−native DNA). For each value of $\Delta_{23,4}$Osm, defined as above using eq 7, $\mu_{23,4}$ was calculated using eq 8. Values of Γ_{μ_3,m_4} were calculated (using eq 6) from values of $\mu_{23,4}$(eq 8) with $\mu_{33,4}$ approximated by $\mu_{33}(m_3)$.

Values of $\mu_{33}(m_3)$ were obtained according to eq 9B by differentiating the best-fitted functional form of Osm(m_3) with respect to m_3 obtained from our VPO data and literature ID data for GB (*41*) and for urea (*42*). For all the data sets, a quadratic function was found to be sufficient to describe the functional dependence of osmolality on solute molality m_3 at constant m_{2u}, m_4, or both in the concentration ranges of interest (≤2.1 *m* GB, ≤2.4 *m* urea). In each case, the quality of the fitting was assessed by the F_R test and the multiple-correlation coefficient R^2 (*43*), and the F-test for an additional term (*43*) was used to assess the justifiability of linear or cubic fitting functions. For those data sets at identical solution conditions (for example, all two-component urea (or GB) solutions, three-component urea (or GB) solutions at the same fixed salt concentration), global fitting was performed to reduce the random uncertainties. Our fitting procedures are based on multiple linear regression (*43*). Experimental uncertainties in all osmometric readings arising from the standard deviation of the triplicate readings of identical samples and in calibrating the instrument are calculated using eq 10 of ref *19*. Error propagation was performed by applying the formula (3.13) in ref *43*; covariances of correlated parameters were included in error propagation.

To analyze our constant molarity data, conversions from constant molarity to constant molality were performed by assuming a linear dependence of osmolality on m_{2u}, m_4, or both (the ratio of m_{2u}/m_4 being constant) within the range of m_{2u}, m_4, or both encountered in a constant molarity titration. In the range 0.15−1 *m* NaCl, we indeed find that the dependence of osmolality on NaCl molality in the presence of constant molality of GB (0, 0.54, or 1.23 *m*, and $m_{2u} = 0$) is linear, and the slope of Osm vs NaCl molality is approximately the same for 0, 0.54, and 1.23 *m* GB (data not shown). Also, titrations of aqueous DNA/KCl solutions with pure H_2O, maintaining a constant ratio of m_{2u}/m_4 (equal to one of the ratios investigated here, data not shown), confirmed that osmolality varies linearly with m_{2u} (and m_4) within the concentration range and for the ratios m_{2u}/m_4 studied here. Results of analyzing such converted data sets were compared with corresponding constant molality data sets at the same values of m_{2u}, m_4, or both, and no significant differences were found in the resulting values of $\mu_{23,4}$ and Γ_{μ_3,m_4} reported here.

Calculations of Water-Accessible Surface Area (ASA) of DNA and α-Helical Peptide. Calculations of ASA of ds (double-helical) and ss (single-helical or extended unstructured) DNA were performed as previously described (*44*).

Conformations of nucleotides in stacked, single-helical DNA strands are assumed to be the same as their conformations in the double helix. In the extended, unstacked model of the ss state, alternate bases are flipped out from the sugar−phosphate backbone and rotated to varying extents, effectively eliminating all base−base interactions. The sequence GCAC (with its complementary strand for double-stranded B-DNA) built using Insight II (Biosym Technologies) was used to obtain the water-accessible surface area (ASA) for individual atoms of each nucleotide (dA, dT, dG, dC). These ASA results for individual nucleotides were combined appropriately for a given specified GC% (or AT%) to calculate the ASA per nucleotide. An alternative calculation was performed to obtain average ASA per nucleotide for each base type in ds and ss helical DNA, in terms of the context (i.e., nearest neighbors) of the nucleotide. In this model, a sequence of 98 bp B-DNA was first built using Insight II, in which all possible (16) arrangements of the nearest neighbor for each nucleotide (dA, dT, dG, dC) were included. The ASA of this sequence was then calculated using the program ANAREA (*45*). The ASA of a nucleotide was obtained by averaging its ASA in the 16 triplets representing all possible arrangements of nearest neighbors. Total ASA per nucleotide from these two model calculations agree within 4% for DNA of 0%, 50%, or 100% GC.

The negatively charged ASA in DNA is the sum of ASA of two oxygens connected to each phosphate by partial double bonds. The polar ASA of DNA is the sum of ASA of all oxygens (other than the negatively charged phosphate oxygens) and nitrogens. The amount of polar amide ASA of a DNA base is defined as the ASA of those nitrogen and carbonyl oxygens found in amide-like functional groups: N1, O2, N3, and O4 of thymine; N1, N3, and O2 of cytosine; N1 and O6 of guanine. No nitrogen or oxygen in adenine fits this criterion. The nonpolar ASA in DNA is the sum of ASA of carbons. ASA per nucleotide for polar, nonpolar, and charged surfaces in ds and ss helical DNA at 0, 50, or 100% GC, obtained from these two models, agree in most cases within ∼5%; an exception is a ∼15% difference in calculated polar ASA in 100% AT ss helical DNA. These differences are not significant for the semiquantitative conclusions of our ASA analysis. Compositions of the ASA of ds DNA and of half-stacked ss DNA, as well as of the ΔASA in the conversion of ds DNA to half-stacked ss DNA for DNA of 50%GC is listed in Table 1. These values are not significantly dependent on base composition.

The previously described (*4*) calculation of ASA for the native state of alanine-based α-helical peptide was revised as follows. The original model of the α-helix, obtained using Insight II, buries some carboxylate oxygen surface as a consequence of a presumably nonphysical packing of carboxylate oxygens of glutamate side chains against the hydrophobic part of the lysine side chains. We revised this model to make the glutamate side chains fully solvent-accessible. The actual helical structure in solution presumably has some contribution from ion pairing of glutamates and lysines, the extent of which is presently not known. The composition of native BSA and native HEWL surface and of the surface exposed in unfolding lacI HTH (*66*) or unfolding alanine-based α-helical peptide is also listed in Table 1 for comparison.

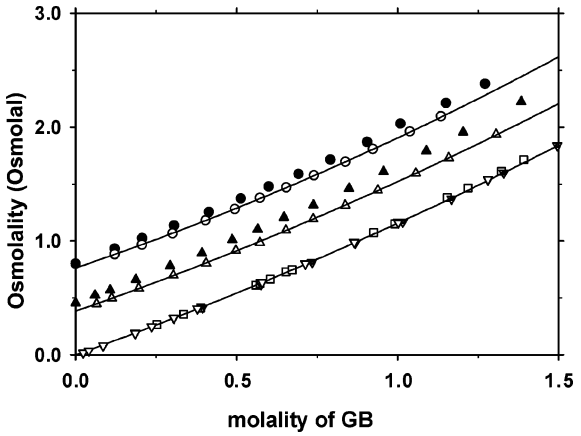

FIGURE 1: Glycine betaine−ds DNA interactions characterized by VPO at 25 or 37 °C. Representative VPO determinations of the effect of native calf thymus DNA on the GB dependence of osmolality at constant molality of KCl are presented. Osmolality is plotted versus GB molality (m_3) for paired series at 0.427 *m* KCl (●, 0.106 mono-*m* DNA; ○, no DNA) and at 0.212 *m* KCl (▲, 0.203 mono-*m* DNA; △, no DNA) and for a two-component GB−water solution (▽ for VPO data and □ for ID data (*41*)). Different shadings of downward triangles represent different data sets. Each VPO data point is the average of triplicate readings on identical samples; the uncertainty is approximately the size of the plotted point. The lines are the best quadratic fits of osmolality vs m_3 for GB−KCl−water data at KCl molality of 0.427, 0.212, and 0 *m*, respectively.

RESULTS

The Presence of DNA Greatly Amplifies the Osmotic Effect of Adding Glycine Betaine (but Not Urea) to a Salt Solution. Figure 1 compares VPO determinations of the osmotic effects of adding various molalities of GB to solutions containing fixed molalities of KCl and DNA (0 *m* KCl and 0 *m* DNA; 0.212 *m* KCl with or without 0.203 *m* (m_{2u}) KDNA; 0.427 *m* KCl with or without 0.106 *m* (m_{2u}) KDNA). The nearly parallel curves drawn through the open symbols in Figure 1 are the best fitted quadratic functions for the dependence of the osmolality of aqueous GB solutions on GB molality in the absence of KCl (current VPO data, open inverted triangles; literature ID data, *41*, open squares) or in the presence of 0.212 *m* (open triangles) or 0.427 *m* (open circles) KCl. Osmolalities of the corresponding GB−DNA−KCl solutions as a function of GB molality are shown by the corresponding solid symbols. Figure 1 shows that simultaneous presence of GB and DNA at DNA concentrations of 0.1 *m* (solid circles) and especially 0.2 *m* (solid triangles) provides an osmolality boost that increases with increasing GB molality and is larger at the higher DNA molality; this effect is not due to KCl, as evidenced by the near-parallel curves in the absence of DNA for osmolality as a function of GB molality in the presence or absence of KCl.

As shown in Figure 2 for a comparable series of salt and DNA concentrations (using the same symbols for four-, three-, and two-component data at the DNA and salt concentrations of Figure 1), virtually no osmolality boost occurs upon addition of urea to a DNA solution at either 0.212 *m* or 0.427 *m* KCl. The effect of addition of urea on osmolality is virtually the same in the presence or absence of DNA; also, in the absence of DNA, the effect of addition of urea on osmolality is the same in the presence or absence

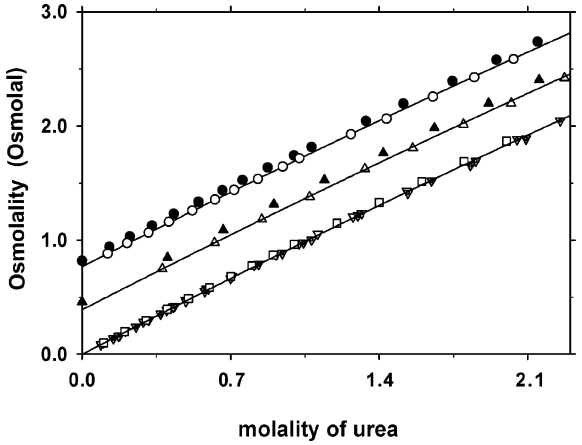

FIGURE 2: Urea−ds DNA interactions characterized by VPO at 25 or 37 °C. Representative VPO determinations of the effect of native calf thymus DNA concentration on the urea dependence of osmolality at constant molality of KCl are presented. Osmolality is plotted versus urea molality (m_3) for paired series at 0.427 *m* KCl (●, at 0.113 mono-*m* DNA; ○, no DNA) and at 0.212 *m* KCl (▲, at 0.197 mono-*m* DNA; △, no DNA) and for a two-component urea−water solution (▽ for VPO data and □ for ID data (*42*)). Different shadings of downward triangles represent different data sets. Each VPO data point is the average of triplicate readings on identical samples; the uncertainty is approximately the size of the plotted point. The lines are the best quadratic fit of osmolality vs m_3 for urea−KCl−water data at KCl molality of 0.427, 0.212, and 0 m, respectively.

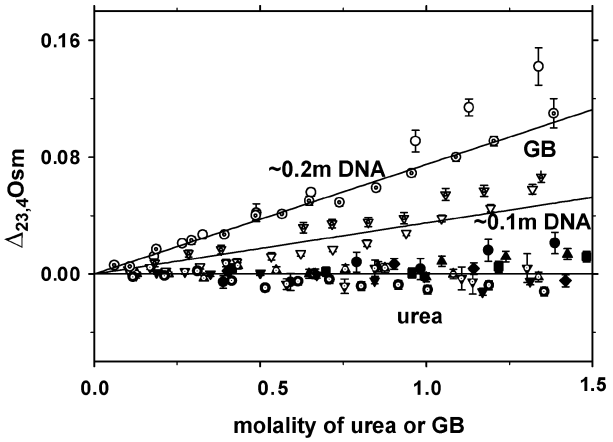

FIGURE 3: Comparison of the effect of the concentration of calf thymus DNA on $\Delta_{23,4}$Osm (see eq 7) for GB and urea. The values of $\Delta_{23,4}$Osm are plotted versus molality of GB or urea (m_3). Open symbols represent data for the GB−DNA−KCl−water system (○, 0.2 *m* DNA; ▽, 0.1 *m* DNA). Different shadings represent different data sets. Closed symbols are for the urea−DNA−KCl−water system: (◆) 0.197 *m* DNA and 0.213 *m* KCl; (■) 0.110 *m* DNA and 0.212 *m* KCl; (▲) 0.120 *m* DNA and 0.427 *m* KCl; (●) 0.213 *m* DNA and 0.427 *m* KCl; (▼) 0.098 *m* DNA and 0.427 *m* KCl; (dotted upward triangles) 0.113 *m* DNA and 0.427 *m* KCl; (dotted downward triangles) 0.104 *m* DNA and 0.427 *m* KCl; (⊙) for 0.221 *m* DNA and 0.427 *m* KCl. The lines are the linear least-squares fit of $\Delta_{23,4}$Osm vs m_3, respectively, for GB system at 0.2 *m* DNA and 0.1 *m* DNA and for urea system (the average slope used here, which is the same for each DNA concentration, 0.2 or 0.1 *m*).

of KCl at the comparatively low concentrations investigated here.

The highly nonadditive effects of GB and contrasting additive effects of urea on osmolality of salt solutions in the presence and absence of DNA are shown in Figure 3 where $\Delta_{23,4}$Osm, defined as in eq 7, is plotted vs solute molality m_3 for the different DNA concentrations investigated. The

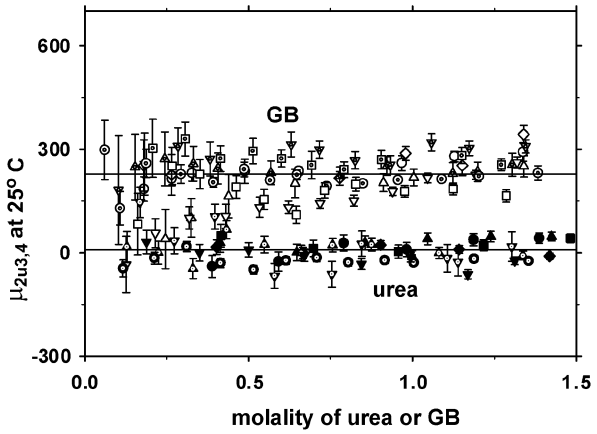

FIGURE 4: Comparison of $\mu_{2u3,4}$ for urea−DNA and GB−DNA interactions as a function of solute concentration. Values of $\mu_{2u3,4}$ (see eqs 8 and 11) at 25 °C are plotted as functions of urea or GB molality (m_3). The open symbols represent data for GB−DNA: (△) 0.184 *m* DNA and 0.364 *m* NaCl; (dotted upward triangles) 0.178 *m* DNA and 0.470 *m* NaCl; (○) 0.214 *m* DNA and 0.212 *m* KCl; (◇) 0.208 *m* DNA and 0.404 *m* KCl; (▽) 0.097 *m* DNA and 0.212 *m* KCl; (dotted squares) 0.106 *m* DNA and 0.427 *m* KCl; (dotted downward triangles) 0.095 *m* DNA and 0.212 *m* KCl; (⊙) 0.203 *m* DNA and 0.212 *m* KCl; (□) 0.098 *m* DNA and 0.427 *m* KCl. The closed symbols represent data for urea−DNA with the same notation as that in Figure 3. The lines are the respective average value of $\mu_{2u3,4}$ for GB (222 cal mol^{-1} *m*$^{-1}$) and urea (4 cal mol^{-1} *m*$^{-1}$) data.

quantity $\Delta_{23,4}$Osm is the difference between the osmotic effect of addition of solute (GB or urea) to a DNA−salt solution and the osmotic effect of the corresponding addition of that solute to a salt solution in the absence of DNA. To evaluate $\Delta_{23,4}$Osm, individual values of Osm(m_2,m_3,m_4) were the directly measured VPO data points (see Methods). For GB, $\Delta_{23,4}$Osm is positive and increases with increasing concentrations of DNA and GB. For urea, $\Delta_{23,4}$Osm is very slightly positive (equal to zero within the uncertainty) at all DNA and urea concentrations investigated; at each DNA concentrationm the average slope is 0.002 ± 0.002 for the fitting of $\Delta_{23,4}$Osm vs m_3 with fixed zero intercept.

Determination of the Effect of Glycine Betaine or of Urea on the Chemical Potential of DNA. To quantify the chemical potential derivatives $\mu_{2u3,4}$ of DNA (expressed per nucleotide monomer) as a function of GB or urea molality, values of $\Delta_{23,4}$Osm (cf. Figure 3) were introduced into eq 8. All the fitting functions for three- and two-component solutions are listed in the appended table (Table A1**)**. In an accompanying table (Table A2), an example of the evaluation of $\Delta_{23,4}$Osm and $\mu_{2u3,4}$ is given for GB−DNA with uncertainties shown for each stage.

The signs and magnitudes of $\mu_{2u3,4}$ characterize how the chemical potential of DNA in aqueous salt solution depends on the molality of the small solute (GB or urea). In Figure 4, values of $\mu_{2u3,4}$ for GB−DNA and for urea−DNA interactions are plotted versus m_3 for the different specifications of fixed m_{2u} and m_4. For both GB and urea, values of $\mu_{2u3,4}$ obtained at different concentrations of DNA (0.1 or 0.2 *m*) and salt (0.2 or 0.4 *m*) do not show any significant trends. As shown in Figure 4, values of $\mu_{2u3,4}$ for GB−DNA and for urea−DNA differ significantly, though each is independent of solute concentration within uncertainty. For GB−DNA interactions, the average value of $\mu_{2u3,4}$ at 25 °C ($m_3 \leq 1.4$ *m*) is 222 ± 8 cal mol^{-1} *m*$^{-1}$. (The reported

Table 2: Preferential Interaction Coefficients of Glycine Betaine (GB) and of Urea with DNA and with Protein Surfaces

	T (°C)	$\mu_{23,4}$[a] (cal mol^{-1} m^{-1})	$\Gamma_{\mu_3 m_4}/m_3$ [a] (m^{-1})	$10^4 \times (\Gamma_{\mu_3}/(m_3\text{ASA}))$ (m^{-1} Å^{-2})
		GB−DNA		
ds DNA surface	25	222 ± 8	−0.30 ± 0.02	−18 ± 1
surface exposed in DNA melting	40−90[b]		$0.14X_{GC} - 0.013$[c]	$14X_{GC} - 1.3$[c]
		GB−Protein[d]		
folded BSA surface	25	(21.7 ± 3.4) × 10^3	−23.1 ± 1.4	−8.3 ± 0.5
folded HEWL surface	25	(2.8 ± 1.3) × 10^3	−3.1 ± 1.1	−4.7 ± 1.7
surface exposed in unfolding lacI HTH	25			−3.8 ± 0.5
		Urea−DNA		
ds DNA surface	25	4 ± 4	−0.02 ± 0.02	−1 ± 1
surface exposed in DNA melting	25		0.07 ± 0.01[e]	7 ± 1[e]
		Urea−Protein		
folded BSA surface[f]	25		3.9 ± 1.4	1.4 ± 0.5
surface exposed in unfolding lacI HTH[g]	25			2.0 ± 0.1
surface exposed in unfolding alanine-based α-helical peptides[h]	25			8.7 ± 0.3

[a] All values for DNA are per nucleotide. [b] The T_m at $C_3 \rightarrow 0$ is shown, and T range reflects the GC dependence of T_m of DNA. [c] From analysis of literature data (*5*). [d] From Felitsky et al. (*66*). [e] From analysis of literature data (*6*−*8*; converted to 25 °C). [f] From Cannon et al., manuscript in preparation. [g] From ref *1*. [h] From analysis of literature data (*16*; converted to 25 °C).

uncertainty is the standard deviation divided by the square root of the number of data points.) This large positive value of $\mu_{2u3,4}$ for GB−DNA indicates that addition of GB strongly increases the chemical potential of ds DNA. The origin of this effect is presumably not direct (e.g., Coulombic) repulsion of GB from DNA, but rather the preference of both DNA and GB to interact with water rather than with each other. The large increase in the osmotic coefficient of two-component aqueous GB solutions with increasing GB concentration (see Appendix A) indicates that GB prefers to interact with H_2O instead of other GB molecules. For urea−DNA, the average value of $\mu_{2u3,4}$ at 25 °C ($m_3 \leq 1.6$ m) is 4 ± 4 cal mol^{-1} m^{-1}. Because the chemical potential of DNA (μ_{2u}) is only slightly increased by increasing urea concentration, the thermodynamic consequences of the interactions of urea and water with DNA must be very similar. Both the grooves and sugar phosphate backbone of native DNA are extensively hydrated (*30*, *46*, *47*). The preference of both DNA and GB to be hydrated instead of interacting with each other causes local exclusion of GB from the hydration layer of DNA; this exclusion of GB is the origin of the positive $\mu_{2u3,4}$, as discussed below.

Preferential Interaction Coefficients for Glycine Betaine− and Urea−DNA Interactions. Preferential interaction coefficients for solute biopolymer interactions (Γ_{μ_3,m_4}, eq 6) provide quantitative information about the partitioning of solute between the vicinity of the biopolymer surface and the bulk solution when interpreted in the context of solvent exchange (*48*, *49*) or the local−bulk solute partitioning model (*2*, *3*, *17*, *67*). In addition, values of Γ_{μ_3,m_4} for the interactions of a perturbing solute (GB or urea) with native DNA are needed to interpret the effect of changing the concentration of the perturbing solute on a specific protein−DNA binding process in the presence of 1:1 salt (Hong et al., manuscript in preparation). Values of Γ_{μ_3,m_4} for interactions of GB and of urea with ds DNA are calculated (eq 6) from VPO determinations of $\mu_{2u3,4}$ using $\mu_{33,4}$ approximated by $\mu_{33}(m_3)$ (see eq 9B) from two-component osmolality data for urea or GB.

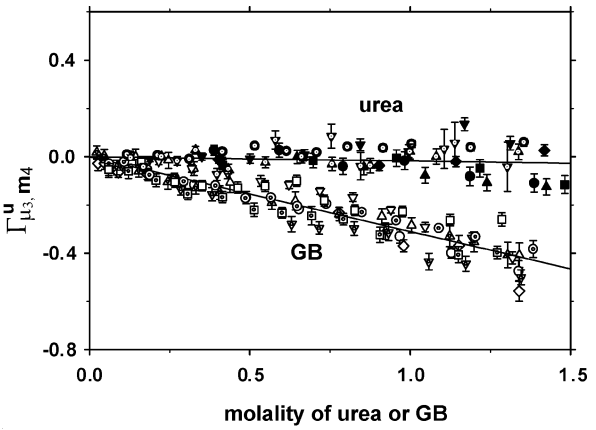

FIGURE 5: Comparison of $\Gamma^u_{\mu_3,m_4}$ for urea−DNA and GB−DNA interactions as a function of solute concentration at 25 °C. Values of $\Gamma^u_{\mu_3,m_4}$ are plotted as functions of urea or GB molality in bulk solution (m_3^{bulk}, calculated by eq 12) for the different specifications of m_{2u} and m_4. The symbol notations are the same as those in Figure 4. Error bars reflect primarily the uncertainty in $\Delta_{23,4}$Osm. Lines with slope $\Gamma^u_{\mu_3,m_4}/m_3^{bulk} = -0.30 \pm 0.02$ for GB−DNA and $\Gamma^u_{\mu_3,m_4}/m_3^{bulk} = -0.02 \pm 0.02$ for urea−DNA are plotted to show the average behavior of the GB−DNA and urea−DNA data sets.

In Figure 5, values of $\Gamma^u_{\mu_3,m_4}$ (eq 11) are plotted against bulk solute molality, m_3^{bulk}, for both GB−DNA and urea−DNA solutions. Propagated uncertainties are primarily determined from uncertainties in $\mu_{2u3,4}$(see Figure 4). For GB, Figure 5 reveals that values of $\Gamma^u_{\mu_3,m_4}$ are negative and increase in magnitude in proportion to m_3^{bulk}; for urea, values of $\Gamma^u_{\mu_3,m_4}$ are approximately zero at all m_3^{bulk} investigated. These values of $\Gamma^u_{\mu_3,m_4}$ indicate that GB is strongly excluded from the vicinity of DNA surface in the presence of 1:1 salt, whereas urea is essentially randomly distributed between the local domain near the DNA surface and the bulk

salt solution. As observed in $\mu_{2u3,4}$ for both GB−DNA and urea−DNA interactions (Figure 4), there is no significant dependence of $\Gamma^u_{\mu_3,m_4}$ on either m_{2u} (0.1 or 0.2 *m*), m_4 (0.2 or 0.4 *m*), or the ratio m_{2u}/m_4 (0.25−1). Since both GB and urea have no net charge under the conditions of these experiments, $\Gamma^u_{\mu_3,m_4}$ must approach zero as m_3 and (hence m_3^{bulk}) approaches zero (cf. ref *50*). At each condition (m_{2u} and m_4) investigated, $\Gamma^u_{\mu_3,m_4}$ is well described as a linear function of m_3^{bulk} with a zero intercept (see Figure 5).

Proportionality constants ($\Gamma^u_{\mu_3,m_4}/m_3^{bulk}$) were determined by linear least-squares fitting (intercept fixed at zero) of $\Gamma^u_{\mu_3,m_4}$ vs m_3^{bulk} for each condition (m_{2u} and m_4) investigated; these were averaged to obtain $\Gamma^u_{\mu_3,m_4}/m_3^{bulk} = -0.30 \pm 0.02$ for GB−DNA and $\Gamma^u_{\mu_3,m_4}/m_3^{bulk} = -0.02 \pm 0.02$ for urea−DNA (see Table 2). The uncertainties were calculated as standard deviations of the slope ($\Gamma^u_{\mu_3,m_4}/m_3^{bulk}$) divided by the square root of the number of data sets averaged (nine for GB and eight for urea).

DISCUSSION

Interactions of Glycine Betaine and of Urea with Native DNA: Comparison with Interactions of these Solutes with Protein Surface. The large negative value of $\Gamma^u_{\mu_3,m_4}/m_3^{bulk}$ for GB−DNA and the very small negative value (comparable to the uncertainty) of $\Gamma^u_{\mu_3,m_4}/m_3^{bulk}$ for urea−DNA demonstrate that GB is strongly excluded from native DNA but urea is only very slightly (if at all) excluded from native DNA. These behaviors contrast with the favorable interactions (accumulation) of these solutes with surface exposed in DNA denaturation, determined here (cf. Table 2) by analyzing literature data. To compare preferential interaction coefficients for interactions of GB or urea with nucleic acid and with folded and unfolded protein surface, values of $\Gamma^u_{\mu_3,m_4}/m_3^{bulk}$ were normalized by the water-accessible surface area (ASA) per nucleotide monomer (171 Å^2) in a B-DNA helix. For a homologous series of biopolymers, with the same surface composition (and therefore the same average hydration b_1° per unit of surface) but differing in ASA, the quantity $\Gamma^u_{\mu_3,m_4}/m_3^{bulk}$ at low m_3^{bulk} is predicted to be directly proportional to biopolymer ASA (*2*, *3*). Urea and GuHCl denaturant *m*-values, shown to be proportional at low m_3^{bulk} to the quantity ($\Gamma^\Delta_{\mu_3}/m_3^{bulk}$) for the surface exposed in unfolding or melting (designated Δ) (*3*), are indeed found to be proportional to the ASA$^\Delta$ exposed in unfolding or melting (*3*, *15*). For native protein surface, the assumption that $\Gamma_{\mu_3}/m_3^{bulk}$ is proportional to ASA is consistent with the available data for globular proteins interacting with a range of excluded and accumulated solutes (*2*, *4*).

Calculated values of the preferential interaction of GB and urea with ds DNA per unit ASA ($\Gamma_{\mu_3,m_4}/(m_3^{bulk}$ASA)) are listed in Table 2, together with the corresponding results for the preferential interactions per unit ASA of these solutes with native protein surface (BSA, HEWL (*66*)) and with the surface exposed in unfolding the lacI HTH (*1*) and alanine-based α-helical peptide (calculated from unfolding data in ref *16* as in ref *3*). If the biopolymer surfaces in Table 2 formed a homologous series with uniform interactions with GB or urea, values of $\Gamma_{\mu_3}/(m_3^{bulk}$ASA) (or $\Gamma_{\mu_3,m_4}/(m_3^{bulk}$ASA)) would be the same for all surfaces. Clearly this is not the case. For GB, with the important exception (discussed below) of the surface exposed upon melting GC base pairs, $\Gamma_{\mu_3}/(m_3^{bulk}$ ASA) becomes increasingly negative as the character of the biopolymer surface changes from the predominantly nonpolar surface exposed in unfolding the lacI HTH to the highly anionic charged surface of native DNA. Indeed values of $\Gamma_{\mu_3}/(m_3^{bulk}$ASA) for GB correlate with the fraction of biopolymer ASA that is anionic oxygen surface (*66*). Therefore, to a first approximation, interactions of GB with native DNA and with native and denatured protein surface can be described as strong exclusion of GB from the water of hydration of anionic oxygen surface and uniform (random) distribution of GB elsewhere. Previous analyses of DNA hydration concluded that hydrogen bonding of water to DNA phosphates is stronger than to bases (*51*), that the extent of hydration of phosphates is larger than the extent of hydration of bases (*46*), and that 85% of all water contacts to phosphate oxygens in crystal structures are due to the two anionic oxygens (*46*).

Per unit of accessible surface area, the preferential interaction of urea with ds DNA surface (quantified by $\Gamma_{\mu_3}/(m_3^{bulk}$ASA)) is smaller in magnitude than its interactions with folded or unfolded protein surface and far smaller than the interactions of GB with native DNA or folded protein surface. The correlation of urea interaction with biopolymer surface composition will be discussed in the following section.

In the solute partitioning model, the preferential interaction coefficient is interpreted in terms of a local−bulk partition coefficient for the distribution of the solute between the biopolymer surface (local domain) and the bulk solution $K_p \equiv m_3^{loc}/m_3^{bulk}$(*2*). At low solute concentrations (≤1−2 *m*):

$$\frac{\Gamma_{\mu_1,\mu_3}}{m_3^{bulk}} \cong \frac{(K_p^\circ - 1)B_1^\circ}{m_1^\bullet} \qquad (13)$$

In eq 13, K_p° is the limiting value of K_p as m_3 approaches zero. For GB−protein interactions, K_p increases with increasing GB concentration as a consequence of the concentration-dependent nonideality exhibited in a two-component aqueous GB solution, which is attenuated upon interaction with the protein surface (*67*). In eq 13, B_1° is the hydration of the biopolymer in the absence of small solute; $B_1^\circ \equiv b_1^\circ$ ASA, where b_1° is the amount of water in the local domain expressed as molecules of water per Å^2 of biopolymer surface; Γ_{μ_1,μ_3} is the dialysis preferential interaction coefficient, which is in general not significantly different in magnitude from Γ_{μ_3} for interactions of small solutes with biopolymers (*52*). From the analysis of VPO data (Figure 5) on the exclusion of GB from DNA (preferential hydration) using the local−bulk solute partitioning model (eq 13), we obtain a minimum estimate of B_1° and hence of DNA hydration by assuming complete exclusion ($K_p^\circ = 0$) of GB from all ds DNA surface: $B_1^\circ \geq 17 \pm 1$ H_2O per nucleotide of ds DNA. At a higher level of resolution, we find that GB is strongly excluded from anionic oxygen surface (44% of total ASA) and moderately from the minimal amount of amide-like surface (2% of total ASA) (*66*) and that GB is randomly distributed (neither excluded nor accumulated) elsewhere. For duplex DNA, the above estimate of B_1° therefore applies only to anionic oxygen surface, and we conclude that the minimum hydration of anionic oxygen

surface is 17 H_2O per nucleotide or 0.22 H_2O Å^{-2} of anionic phosphate oxygen surface, which corresponds to two layers of water (assuming 0.11 H_2O Å^{-2} in a hydration monolayer (*53*, *54*)). If GB were not completely excluded from anionic DNA surface, the hydration of this surface would of necessity exceed 0.22 H_2O Å^{-2}. This result, obtained from analysis of GB−DNA preferential interaction data, is consistent with the finding that two layers of water surrounding nucleic acid surface exhibit a density and compressibility that differ from those of bulk water (*47*).

For the interaction of urea with ds DNA, where $\Gamma^{u}_{\mu_3,m_4}/m_3^{bulk} = -0.02 \pm 0.02$, the partition coefficient K_p° is not significantly less than unity (e.g., $K_p^\circ = 0.94 \pm 0.06$ if the average $b_1 \cong 0.11$ H_2O Å^{-2}), which indicates that the average local concentration of urea in the vicinity of native DNA surface is only slightly less than its bulk concentration. The extremely small preferential interaction of urea with ds DNA implies that any effect of urea on binding of a protein to ds DNA can be interpreted in terms of changes in protein amide surface. Effects of GB on protein DNA interactions (e.g., ref *55*) are predicted to result primarily from changes in hydration of protein anionic carboxylate oxygen surface or of anionic DNA phosphate surface. Comparative studies of the effect of urea and of GB on protein−DNA interactions are in progress to test these predictions.

Interactions of Urea and of Glycine Betaine with Single-Stranded DNA Surfaces. VPO experiments demonstrate that GB is highly excluded from double-stranded (ds) DNA surface, whereas urea is uniformly distributed in a solution of ds DNA. If these solutes were also excluded from the surface exposed in melting DNA, they would both act as DNA stabilizers, as is observed for GB (but of course not for urea) with globular proteins (*66*). However both solutes in general destabilize ds DNA. Urea reduces T_m of various naturally occurring DNA and synthetic polynucleotides by approximately 3 K per molar urea added, up to at least 6 M urea ($dT_m/dC_3 \cong -3$ K M^{-1}) (*6*−*8*); the effect of urea appears independent of DNA base composition (*6*). For comparison, urea reduces T_m of lacI HTH by 6.5 K M^{-1} at low urea concentration, an effect on T_m that is twice as large as that reported for DNA (*1*).

GB reduces T_m of the ds dGC·dGC alternating sequence homopolymer by approximately 6.8 K M^{-1}; the effect of GB is linear up to ∼4 M GB (*5*). At higher GB concentrations the destabilizing effect increases (*5*), as expected from the strong increase in the activity coefficient of GB in this range (*41*, *67*). In contrast, T_m of the ds dAT·dAT alternating sequence homopolymer increases with increasing GB concentration by approximately 0.7 K M^{-1} over the range 0−4 M GB. Naturally occurring ds DNA with intermediate GC compositions ($0.26 \le X_{GC} \le 0.70$) behaves as expected from simple additivity; up to ∼4 M GB, all these data can be represented by $dT_m/dC_3 \cong 0.70 - 7.5X_{GC}$ (*5*).

These literature values of dT_m/dC_3 provide estimates of preferential interaction coefficients for the interactions of GB and of urea with the DNA surface exposed in melting. The initial slope $(dT_m/dC_3)^o$ as C_3 approaches zero is related to the corresponding limiting value (designated by the superscript o) of the solute molality normalized preferential interaction coefficient $(\Gamma^{\Delta}_{\mu_3}/m_3)^o$ of the solute for the surface exposed in melting by the equation (*18*)

$$\left(\frac{dT_m}{dC_3}\right)^o \cong -\frac{RT_m^{\,2}}{\Delta H^\circ_{obs}}\left(\frac{\Gamma^{\Delta}_{\mu_3}}{m_3}\right)^o \qquad (14)$$

Here, in accordance with eq 13 for the solute partitioning (local−bulk domain) model,

$$\left(\frac{\Gamma^{\Delta}_{\mu_3}}{m_3}\right)^o \cong \frac{(K_p^\circ - 1)b_1^\circ \mathrm{ASA}^{\Delta}}{m_1^\bullet} \qquad (15)$$

Equation 14 utilizes values of ΔH°_{obs} and T_m determined in the absence of solute ($RT_m^{\,2}/\Delta H^\circ_{obs} \cong 52$ K for ds DNA melting, which are independent, to a first approximation, of GC composition or salt concentration (*56*−*58*)). Both ΔH°_{obs} and $\Gamma^{\Delta}_{\mu_3}$ are expressed per nucleotide monomer. In eq 15, ASA^{Δ} is the change in water-accessible surface area per nucleotide melted, estimated (as described in Methods) to be 100 Å^2 (see Table 1). For typical in vitro studies of a DNA denaturation process, the m_3 is in large excess of DNA concentration and, hence, not significantly different from m_3^{bulk}. Therefore, to simplify our DNA denaturation analysis, we do not distinguish m_3 from m_3^{bulk}.

Urea. For urea, analysis of the initial slope, $(dT_m/dC_3)^o \cong -3$ K M^{-1}, using eq 14 yields the estimate $(\Gamma^{\Delta}_{\mu_3}/m_3)^o \cong 0.06$ m^{-1}, applicable at temperatures of 60−70 °C. (The uncertainty in $(\Gamma^{\Delta}_{\mu_3}/m_3)^o$ is at least ±20% based on the range of literature results.) Urea is therefore moderately accumulated at the DNA surface exposed upon melting, as expected because it is a DNA denaturant. Correcting this estimate to 25 °C using the temperature dependence of the preferential interaction of urea with protein surface (*1*) yields for urea−DNA $(\Gamma^{\Delta}_{\mu_3}/m_3)^o \cong 0.07 \pm 0.01$ m^{-1}. Assuming that 100 Å^2 of DNA surface is exposed in melting (see Table 1), $\Gamma^{\Delta}_{\mu_3}/(m_3\mathrm{ASA}^{\Delta}) \cong 7 \times 10^{-4}$ m^{-1} Å^{-2}. Interpretation of $\Gamma^{\Delta}_{\mu_3}/(m_3\mathrm{ASA}^{\Delta})$ using the solute partitioning model (*2*), assuming an average hydration of the DNA surface exposed upon melting $b_1 = 0.11$ H_2O Å^{-2}, yields a local−bulk urea partition coefficient $K_p^\circ \cong 1.35$. Therefore, the average local concentration of urea at the nucleotide surface exposed on melting exceeds its bulk concentration by ∼35%. By comparison the average local concentration of urea in the vicinity of both folded BSA and the surface exposed in unfolding lacI HTH is only 10% greater than bulk ($K_p^\circ \approx 1.1$) (*1*, Cannon et al., manuscript in preparation)). No contradiction exists between the fact that experimental values of $(dT_m/dC_3)^o$ are larger for protein unfolding than for DNA melting, and the fact that values of $\Gamma^{\Delta}_{\mu_3}/(m_3\mathrm{ASA}^{\Delta})$ and K_p° are larger for the interaction of urea with the surface exposed on DNA melting than with the surface exposed on protein unfolding. These differences are reconciled by eq 14, because the transition enthalpy, normalized per unit area of surface exposed on melting, is much larger for nucleic acid melting (∼40 cal Å^{-2} at $T_m = 320$ K (*44*)) than for protein unfolding (∼7 cal Å^{-2} for lacI HTH at $T_m = 320$ K (*1*)). Effects of urea on the equilibrium constant for helix formation in short RNA oligomers (*68*) appear consistent with this analysis.

Glycine Betaine. For GB, analysis of the initial slopes $(dT_m/dC_3)^o$ for dAT and dGC homopolymers (*5*) by eq 14 yields $(\Gamma^{\Delta}_{\mu_3,AT}/m_3)^o = -0.013$ (i.e., modest exclusion of GB from AT surface exposed on melting at ∼40 °C) and

$(\Gamma^{\Delta}_{\mu_3,GC}/m_3)^o = 0.13$ (i.e., accumulation of GB at GC surface exposed on melting at ~90 °C) (see Table 2). These effects appear to be additive for all base compositions of naturally occurring DNA (5), analysis of which by eq 14 yields $(\Gamma^{\Delta}_{\mu_3,DNA}/m_3)^o \cong 0.13(1.1X_{GC} - 0.1)$, valid at the T_m (see Table 2). (Independent data for the effect of GB on T_m of calf thymus DNA (*59*) are consistent with this result.) Interpretation of values of $(\Gamma^{\Delta}_{\mu_3}/m_3)^o$ for effects of GB on melting of AT and GC base pairs using eq 15 is performed using the same assumption as for the analysis of urea effects above ($b_1 = 0.11$ H_2O Å^{-2} for the ~100 Å^2 DNA surface exposed in melting). This calculation yields $K^{\circ}_p \cong 0.9$ (i.e., modest exclusion) for the distribution of GB in vicinity of AT surface exposed in melting and $K^{\circ}_p \cong 1.7$ (i.e., significant accumulation) for the distribution of GB in the vicinity of GC surface exposed in melting. The modest exclusion of GB from the AT surface exposed on melting is consistent with that predicted from the polar amide surface of A and T (*66*); strong exclusion of GB from anionic phosphate oxygen surface is not expected to contribute to this effect because the exposure of phosphate surface to water does not increase on melting. The molecular basis of accumulation of GB in the vicinity of GC surface exposed on melting, which we propose must account for the isostabilizing effect (*5*) of GB, has not been determined. Work is in progress to determine K°_p more accurately for the interactions of these solutes with the surface exposed in nucleic acid conformational transitions.

Analysis of Urea Effect on DNA Stability as a Test of the Proposal That Preferential Accumulation of Urea Occurs at Polar Amide Surface. We find that urea is very slightly (if at all) excluded from native DNA surface but is significantly accumulated at the surface exposed in DNA melting. Per unit of ASA, the much more favorable interaction of urea with the base surface exposed in melting than with native DNA surface correlates with the fraction of DNA surface consisting of polar amide-like ASA but not with the fraction consisting of nonpolar or charged ASA (cf. Table 1). Our observation of this correlation is consistent with our proposal (*3*) based on protein data that urea interacts predominantly with polar peptide surfaces on proteins. In Figure 6, the quantity $\Gamma_{\mu_3}/(m_3^{bulk}ASA)$, describing the interaction (per unit ASA) of urea with various surfaces, native BSA or DNA, exposed in unfolding DNA or lacI HTH, or predominantly alanine α-helical peptides (cf. Tables 1 and 2), is plotted against the fraction of polar amide ASA. The value of $\Gamma_{\mu_3}/(m_3^{bulk}ASA)$ for the surface exposed in unfolding α-helical peptides was calculated using the unfolding data at 0 °C in ref *16* and converted to 25 °C using the temperature dependence of the preferential interaction of urea with protein surface (*1*). A strong correlation between $\Gamma_{\mu_3}/(m_3^{bulk}ASA)$ and the fraction of polar amide ASA ($f_{polar\ amide}$) for all types of protein and DNA surfaces investigated is demonstrated by the fact that all data points in Figure 6 can be fitted well to a straight line: $\Gamma_{\mu_3}/(m_3^{bulk}ASA) \times 10^3 = (-0.04 \pm 0.02) + (1.62 \pm 0.07)f_{polar\ amide}$ with $R^2 = 0.99$. Therefore, urea interaction per unit ASA is approximately proportional to the fraction of polar amide ASA, and the polar amide-like ASA of DNA bases behaves the same as the polar amide ASA of protein or peptide surface in its interactions with urea. The intercept is so small that any

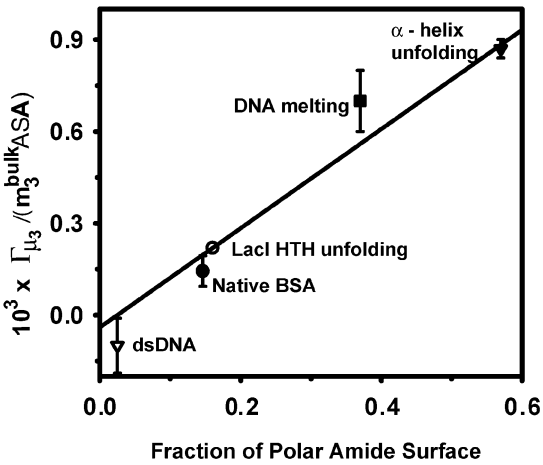

FIGURE 6: Correlation of urea interaction with the fraction of polar amide surface ($f_{polar\ amide}$) in protein and DNA. Values of $10^3 \times (\Gamma_{\mu_3}/(m_3^{bulk}ASA))$ determined or corrected to 25 °C are plotted versus $f_{polar\ amide}$ for ds DNA (▽), native BSA (●), unfolding lacI HTH (○), DNA melting (■), and unfolding α-helical peptide (▼). The error bar indicates the uncertainty in $10^3 \times (\Gamma_{\mu_3}/(m_3^{bulk}ASA))$. The best fit straight line is $10^3 \times (\Gamma_{\mu_3}/(m_3^{bulk}ASA)) = (-0.04 \pm 0.02) + (1.62 \pm 0.07)f_{polar\ amide}$.

contribution from preferential interactions with other types of surface must not be significant compared with polar amide surface. To test this correlation further, correlations analogous to that shown in Figure 6 (not shown) were examined for other types of ASA. Values of $\Gamma_{\mu_3}/(m_3^{bulk}ASA)$ are not proportional to the fraction of nonpolar ASA nor to other polar ASA or charged ASA. The conclusion in Figure 6 is consistent with the long-standing but not universally accepted proposal that the interaction between urea and peptide groups makes a major contribution to the effectiveness of urea as a denaturant of proteins and α-helices (e.g., refs *16* and *60*−*62*). Our results provides no support for the proposal from some analyses of model compound data that the interaction of urea with nonpolar side chains plays a significant role in urea denaturation of proteins (e.g., refs *63*−*65*). Assuming proportionality of $\Gamma_{\mu_3}/(m_3^{bulk}ASA)$ to $f_{polar\ amide}$, we obtain $(K^{\circ}_p - 1)b_1^{\circ} \cong (9.0 \pm 0.4) \times 10^{-2}$ for the interaction of urea with polar amide surface. If the hydration of polar amide surface is a monolayer of water, then $K^{\circ}_p = 1.82$ and urea is accumulated at polar amide surface at a concentration that is 1.82 times its bulk concentration. This information will allow urea to be used as a selective perturbant and a quantitative probe of processes in which the amount of water-accessible polar amide surface changes (Hong et al., Kontur et al., manuscripts in preparation).

ACKNOWLEDGMENT

We thank Peter von Hippel and the referees for their comments on the manuscript, and we thank Irina Shkel, Ming-Fong Lye, and Jonathan Cannon for helpful discussions.

APPENDIX A

VPO Results and Analysis of Osmolalities of Two-Component Glycine Betaine or Urea Solutions and of Three-Component Glycine Betaine−*KCl (or NaCl) Solutions.* To test the accuracy of VPO in measuring osmolality over the range 0.1−2.5 Osm, comparisons were made (cf. Figures 1

Table A1: Concentration Dependence of Osmolality in Aqueous Solutions of Urea or GB and KCl or NaCl

concentrations (m)		fitting function, Osm $= \alpha + \beta m_3 + \gamma m_3^2$ with covariances $\sigma_{\alpha\beta}^2$, $\sigma_{\alpha\gamma}^2$, and $\sigma_{\beta\gamma}^2$.					
KCl or NaCl	urea or GB	α	β	γ	$2\sigma_{\alpha\beta}^2 \times 10^{-5}$	$2\sigma_{\alpha\gamma}^2 \times 10^{-5}$	$2\sigma_{\beta\gamma}^2 \times 10^{-5}$
			KCl−GB				
0.212	0−1.85	0.384 ± 0.001	0.984 ± 0.002	0.154 ± 0.002	−0.29	0.17	−0.87
0.427	0.27−1.23	0.764 ± 0.002	0.958 ± 0.007	0.185 ± 0.005	−2.5	1.7	−6.8
0.404	0−1.91	0.727 ± 0.002	0.971 ± 0.008	0.166 ± 0.005	−3.0	1.6	−8.0
			NaCl−GB				
0.210	0−1.45	0.392 ± 0.001	0.960 ± 0.005	0.169 ± 0.004	−1.2	0.7	−4.0
0.364	0.02−1.34	0.678 ± 0.003	0.953 ± 0.018	0.153 ± 0.015	−9.3	3.7	−52
0.470	0−1.30	0.856 ± 0.002	0.906 ± 0.012	0.184 ± 0.012	−3.2	2.6	−27
			GB−H_2O, ID Data (*41*) and VPO Data				
0	0.023−2.1	0	1.010 ± 0.001	0.157 ± 0.001			−0.056
			KCl−Urea				
0.212	0.1−2.3	0.386 ± 0.002	0.971 ± 0.004	−0.034 ± 0.002	−1.2	0.48	−1.4
0.427	0.1−2.3	0.768 ± 0.001	0.950 ± 0.002	−0.026 ± 0.001	−0.22	0.1	−0.43
			Urea−H_2O, ID Data (*42*) and VPO Data				
0	0.1−2.4	0	0.990 ± 0.001	−0.030 ± 0.001			−0.06

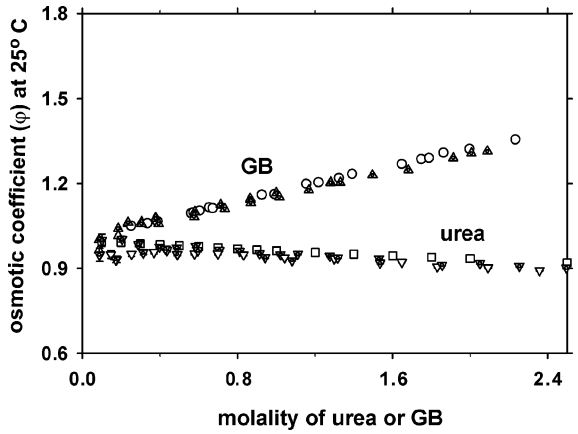

FIGURE A1: Comparison of osmotic coefficients of two-component aqueous solution of GB and of urea at 25 or 37 °C. Osmotic coefficients are plotted versus molality (m_3) of GB or urea for VPO data (▽) and ID data (*42*) (□) for urea and VPO data (△) and ID data (*41*) (○) for GB. Different shadings represent different data sets. The error bars are approximately the size of the plotted point.

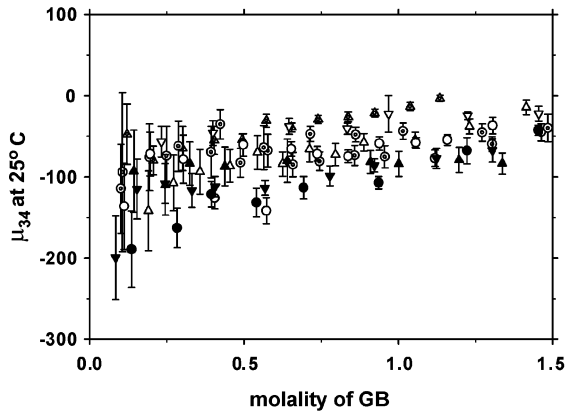

FIGURE A2: μ_{43} as a function of GB concentration at 25 °C for aqueous salt solutions (in the absence of DNA). Values of μ_{43} are plotted versus molality (m_3) of GB. Open symbols represent data sets for GB−KCl: (△) 0.427 *m* KCl; (▽) 0.404 *m* KCl; (○) 0.212 *m* KCl. Closed symbols represent data sets for GB−NaCl: (▲) 0.364 *m* NaCl; (▼) 0.470 *m* NaCl; (●) 0.211 *m* NaCl. Different shadings represent different data sets. Error bars are propagated from the uncertainties in Δ_{43}Osm. The unit of μ_{43} is cal mol^{-1} m^{-1}.

and 2) between osmolalities of aqueous GB or urea two-component solutions determined by VPO in this study and values determined from literature data obtained by isopiestic distillation (ID; ref *41* for GB, ref *42* for urea). For both urea and GB, the VPO and ID data agree well, as also is indicated by the comparison of osmotic coefficients from VPO and ID data shown in Figure A1. Comparison of osmotic coefficients of aqueous two-component solutions containing either GB or urea as functions of their respective molalities reveals the same pattern of interactions as that deduced from Figures 1 and 2 for the preferential interactions of these solutes with DNA. Osmotic coefficients (Figure A1) are greater than unity and increase strongly with increasing GB concentration ($\phi = 1.3$ at $m_3 = 2$ *m*), indicating the strong preference of GB to interact with water rather than with itself. By contrast, in aqueous urea solutions (see Figure A1), ϕ is slightly less than unity in the concentration range of interest (e.g., $\phi = 0.93$ at 2 *m* urea), indicating that effects of favorable urea−urea interactions slightly outweigh effects of urea−water interactions.

To analyze the GB effect on a protein−DNA binding process in the presence of 1:1 salt (Hong et al., manuscript in preparation), we report here values of Γ_{μ_3} characterizing GB−salt interactions obtained by applying eqs 4 and 5 (with index 2 substituted by 4) for the VPO data of GB−H_2O and GB−K(or Na)Cl−H_2O solutions (cf. Figures 1 and 2). In calculations of Δ_{43}Osm as defined by analogy to eq 4, values of Osm(m_3,m_4) were used directly, the value of Osm(m_4) was extrapolated from the fitting function Osm(m_3,m_4) vs m_3 (shown in Table A1) to $m_3 = 0$, and to obtain Osm(m_3), the fitting function Osm(m_3) vs m_3 (shown in Table A1) was interpolated to the same value of m_3 as in Osm(m_3,m_4). Values of Δ_{43}Osm were then applied to eq 5 to calculate μ_{43}, and finally the second equality of eq 2 ($\Gamma_{\mu_3} = -\mu_{43}/\mu_{33}$) was used to calculate Γ_{μ_3} with μ_{33} calculated from μ_{43} via the Gibbs−Duhem linkage (see eq 2 of ref *19*).

Over the range of GB concentrations examined ($\leq$1.5 *m*), values of μ_{43} for both GB−KCl and GB−NaCl interactions, as shown in Figure A2, are negative and significantly larger in magnitude than the contribution due to ideal mixing μ_{43}^{mix} (see ref *19* and Appendix B) (e.g., $\mu_{43} \approx -85 \pm 28$ cal mol^{-1} m^{-1} at 0.5 *m* GB, whereas $\mu_{43}^{mix} \approx -20$ cal mol^{-1} m^{-1} over the range $m_3 \leq 1.5$ *m*), which indicates favorable interaction between GB and salt (KCl or NaCl). Γ_{μ_3} for the interaction of GB with KCl or NaCl is plotted vs GB molality m_3 in

Table A2: Representative Calculation from VPO Data of $\mu_{2u3,4}$ and $\Gamma^{u}_{\mu_3,m_4}$ for GB−DNA at 0.212 *m* KCl, and 0.203 *m* DNA Phosphate

m_3 (*m*)	Osm(m_2,m_3,m_4) (Osm)	Osm(m_3,m_4) (Osm)	$\Delta_{23,4}$Osm (Osm)	$\mu_{2u3,4}$[a] (cal mol^{-1} *m*$^{-1}$)	$\mu^{mix}_{2u3,4}$ (cal mol^{-1} *m*$^{-1}$)	$\mu^{ex}_{2u3,4}$ (cal mol^{-1} *m*$^{-1}$)	$\Gamma^{u}_{\mu_3,m_4}$
0.060	0.523 ± 0.001	0.444 ± 0.001	0.006 ± 0.002	298 ± 86	−10.6	309 ± 86	−0.03 ± 0.01
0.107	0.569 ± 0.001	0.491 ± 0.001	0.005 ± 0.002	129 ± 48	−10.6	140 ± 48	−0.02 ± 0.01
0.187	0.662 ± 0.002	0.573 ± 0.000	0.017 ± 0.003	259 ± 41	−10.6	269 ± 41	−0.08 ± 0.01
0.293	0.781 ± 0.002	0.686 ± 0.000	0.023 ± 0.003	228 ± 27	−10.5	239 ± 27	−0.10 ± 0.01
0.392	0.893 ± 0.001	0.793 ± 0.000	0.027 ± 0.002	204 ± 14	−10.5	215 ± 14	−0.12 ± 0.01
0.486	1.011 ± 0.003	0.898 ± 0.000	0.040 ± 0.003	242 ± 21	−10.5	253 ± 21	−0.17 ± 0.01
0.565	1.103 ± 0.001	0.990 ± 0.001	0.041 ± 0.002	210 ± 10	−10.5	220 ± 10	−0.17 ± 0.01
0.647	1.207 ± 0.003	1.084 ± 0.001	0.050 ± 0.003	226 ± 14	−10.5	236 ± 14	−0.21 ± 0.01
0.738	1.316 ± 0.002	1.194 ± 0.001	0.049 ± 0.003	193 ± 10	−10.4	203 ± 10	−0.20 ± 0.01
0.849	1.462 ± 0.002	1.331 ± 0.001	0.059 ± 0.002	201 ± 9	−10.4	212 ± 9	−0.23 ± 0.01
0.956	1.608 ± 0.002	1.466 ± 0.001	0.069 ± 0.002	211 ± 7	−10.4	221 ± 7	−0.26 ± 0.01
1.089	1.791 ± 0.003	1.638 ± 0.001	0.080 ± 0.003	213 ± 8	−10.4	224 ± 8	−0.30 ± 0.01
1.203	1.955 ± 0.003	1.791 ± 0.001	0.091 ± 0.003	222 ± 8	−10.4	232 ± 8	−0.33 ± 0.01
1.384	2.223 ± 0.010	2.041 ± 0.001	0.110 ± 0.01	231 ± 1	−10.3	241 ± 21	−0.38 ± 0.04
0	0.457 ± 0.001	0.384 ± 0.001					

[a] Uncertainties in $\mu_{2u3,4}$ arise primarily from $\Delta_{23,4}$Osm.

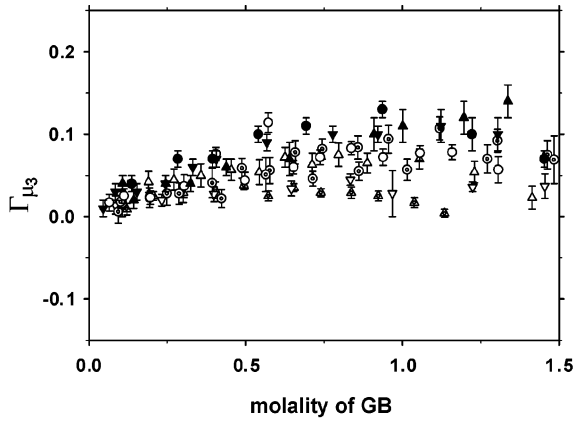

FIGURE A3: Preferential interaction coefficients (Γ_{μ_3}) as a function of GB concentration at 25 °C for aqueous salt solutions (in the absence of DNA). Values of Γ_{μ_3} are plotted versus molality (m_3) of GB. The symbol notations are the same as those in Figure A2. Error bars are propagated from the uncertainties in μ_{43}.

Figure A3, which shows positive values of Γ_{μ_3} for both KCl and NaCl under all conditions investigated. As revealed by Figures A2 and A3, values of both μ_{43} and Γ_{μ_3} are very similar for both GB−KCl and GB−NaCl, and these values do not show any m_4-dependence. The initial slopes of Γ_{μ_3} vs m_3, estimated for GB−KCl and GB−NaCl, are 0.08 ± 0.01 and 0.16 ± 0.01 m^{-1}, respectively.

APPENDIX B

Ideal and Nonideal Contributions to $\mu_{2u3,4}$. The preferential interaction coefficient Γ_{μ_3,m_4} is of importance and of interest because of its relation, through a type of Wyman linkage (*20*, also see eq 1), to the effect of a perturbing solute on K_{obs} of a biopolymer process and its molecular interpretation by the local−bulk domain model. In eq 6, Γ_{μ_3,m_4} is expressed as the quotient of $\mu_{23,4}$ with respect to $\mu_{33,4}$; $\mu_{23,4}$ characterizes the effect of component 3 on the chemical potential of component 2, which is the primary gauge of the preferential interactions between components 2 and 3. To separate the ideal mixing effect from the effect of nonideality on $\mu_{23,4}$, the ideal mixing contribution to $\mu_{23,4}$ is calculated as follows (*50*):

$$\mu^{mix}_{23,4} = -\frac{RT(1+N_u)}{m^{\bullet}_1 + (1+N_u)m_2 + m_3 + 2m_4} \qquad (A1)$$

in which N_u is the average number of nucleotides per DNA molecule. Values of $\mu^{mix}_{2u3,4} \equiv \mu^{mix}_{23,4}/N_u$ are −10 to −11 cal mol^{-1} *m*$^{-1}$ at 25 °C over the range $m_3 \leq 1.6$ *m* for any type of solute 3. The contribution due to nonideality, $\mu^{ex}_{2u3,4}$, is the difference:

$$\mu^{ex}_{2u3,4} = \mu_{2u3,4} - \mu^{mix}_{2u3,4} \qquad (A2)$$

For urea−DNA interactions, the average value of $\mu_{2u3,4}$ (4 cal mol^{-1} *m*$^{-1}$) is comparable to $\mu^{mix}_{2u3,4}$, and hence, $\mu^{ex}_{2u3,4} \approx 0$, which indicates that the mole fraction scale activity coefficient of DNA is not significantly affected by addition of urea in this concentration range. At a molecular level, this means that the interaction of urea with DNA is comparable in strength to the interaction of solvent water with DNA under the conditions investigated. By contrast, for the GB−DNA interaction, the value of $\mu_{2u3,4}$ (222 cal mol^{-1} *m*$^{-1}$) is much larger than $\mu^{mix}_{2u3,4}$, and therefore approximately equal to $\mu^{ex}_{2u3,4}$ (see Table A2). Addition of GB to a DNA solution causes a large increase in the chemical potential and activity coefficient of DNA, implying that GB and DNA both interact much more favorably with water than they do with each other.

REFERENCES

1. Felitsky, D. J., and Record, M. T., Jr. (2003) Thermal and urea-induced unfolding of the marginally stable lac repressor DNA-binding domain: a model system for analysis of solute effects on protein processes, *Biochemistry 42*, 2202−2217.
2. Courtenay, E. S., Capp, M. W., Anderson, C. F., and Record, M. T., Jr. (2000) Vapor pressure osmometry studies of osmolyte-protein interactions: implications for the action of osmoprotectants in vivo and for the interpretation of "osmotic stress" experiments in vitro, *Biochemistry 39*, 4455−4471.
3. Courtenay, E. S., Capp, M. W., Saecker, R. M., and Record, M. T., Jr. (2000) Thermodynamic analysis of interactions between denaturants and protein surface exposed on unfolding: interpretation of urea and guanidinium chloride m-values and their correlation with changes in accessible surface area (ASA) using preferential interaction coefficients and the local-bulk domain model, *Proteins: Struct., Funct., Genet. 41* (S4), 72−85.
4. Courtenay, E. S., Capp, M. W., and Record, M. T., Jr. (2001) Thermodynamics of interactions of urea and guanidinium salts with protein surface: relationship between solute effects on protein processes and changes in water-accessible surface area, *Protein Sci. 10*, 2485−2497.

5. Rees, W. A., Yager, T. D., Korte, J., and von Hippel, P. H. (1993) Betaine can eliminate the base pair composition dependence of DNA melting, *Biochemistry 32*, 137−144.
6. Babayan, Y. S. (1988) Conformation and thermostability of double-helical nucleic acids in aqueous solutions of urea, *Mol. Biol. 22*, 1204−1210.
7. Aslanyan, V. M., Babayan Y. S., and Arutyunyan, S. G. (1984) Conformation and thermal stability of DNA in aqueous urea solutions, *Biophysics 29*, 410−414.
8. Klump, H., and Burkart, W. (1977) Calorimetric measurements of the transition enthalpy of DNA in aqueous urea solutions, *Biochim. Biophys. Acta 475*, 601−604.
9. Fang, X., Littrell, K., Yang, X. J., Henderson, S. J., Siefert, S., Thiyagarajan, P., Pan, T., and Sosnick, T. R. (2000) Mg2+-dependent compaction and folding of yeast tRNAPhe and the catalytic domain of the B. subtilis RNase P RNA determined by small-angle X-ray scattering, *Biochemistry 39* (36), 11107−11113.
10. Timasheff, S. N. (1998) Control of protein stability and reactions by weakly interacting cosolvents: the simplicity of the complicated, *Adv. Protein Chem. 51*, 355−432.
11. Timasheff, S. N., and Xie, G. (2003) Preferential interactions of urea with lysozyme and their linkage to protein denaturation, *Biophys. Chem. 105*, 421−448.
12. Waldner, J. C., Lahr, S. J., Edgell, M. H., and Pielak, G. J. (1999) Nonideality and protein thermal denaturation, *Biopolymers 49*, 471−479.
13. Weatherly, G. T., and Pielak, G. J. (2001) Second virial coefficients as a measure of protein−osmolyte interactions, *Protein Sci. 10* (1), 12−16.
14. Zhang, W., Capp, M. W., Bond, J. P., Anderson, C. F., and Record, M. T., Jr. (1996) Thermodynamic characterization of interactions of native bovine serum albumin with highly excluded (glycine betaine) and moderately accumulated (urea) solutes by a novel application of vapor pressure osmometry, *Biochemistry 35*, 10506−10516.
15. Myers, J. K., Pace, C. N., and Scholtz, J. M. (1995) Denaturant *m* values and heat capacity changes: relation to changes in accessible surface areas of protein unfolding, *Protein Sci. 4*, 2138−2148.
16. Scholtz, J. M., Barrick, D., York, E. J., Stewart, J. M., and Baldwin, R. L. (1995) Urea unfolding of peptide helices as a model for interpreting protein unfolding, *Proc. Natl. Acad. Sci. U.S.A. 92* (1), 185−189.
17. Record, M. T., Jr., and Anderson, C. F. (1995) Interpretation of preferential interaction coefficients of nonelectrolytes and of electrolyte ions in terms of a two-domain model, *Biophys. J. 68*, 786−794.
18. Record, M. T., Jr., Zhang, W., and Anderson, C. F. (1998) Analysis of effects of salts and uncharged solutes on protein and nucleic acid equilibria and processes: a practical guide to recognizing and interpreting polyelectrolyte effects, Hofmeister effects, and osmotic effects of salts, *Adv. Protein Chem. 51*, 281−353.
19. Hong, J., Capp, M. W., Anderson, C. F., and Record, M. T. (2003) Preferential interactions in aqueous solutions of urea and KCl, *Biophys. Chem. 105* (2−3), 517−532.
20. Wyman, J. (1964) Linked functions and reciprocal effects in hemoglobin: a second look, *Adv. Protein Chem. 19*, 223−286.
21. Robinson, R. A., and Stokes, R. H. (1961) Activity coefficients in aqueous solutions of sucrose, mannitol and their mixtures at 25 °C, *J. Phys. Chem. 65* (11), 1954−1958.
22. Bower, V. E., and Robinson, R. A. (1963) The thermodynamics of the ternary system: urea-sodium chloride-water at 25 °C, *J. Phys. Chem. 67*, 1524−1527.
23. Wang, L., Ferrari, M., and Bloomfield, V. A. (1990) Large-scale preparation of mononucleosomal DNA from calf thymus for biophysical studies, *BioTechniques 9*, 24−27.
24. Padmanabhan, S., Zhang, W., Capp, M. W., Anderson, C. F., and Record, M. T., Jr. (1997) Binding of cationic (+4) alanine- and glycine-containing oligopeptides to double-stranded DNA: thermodynamic analysis of effects of Coulombic interactions and alpha-helix induction, *Biochemistry 36* (17), 5193−5206.
25. Stein, V. M., Bond, J. P., Capp, M. W., Anderson, C. F., and Record, M. T., Jr. (1995) Importance of Coulombic end effects on cation accumulation near oligoelectrolyte B-DNA: a demonstration using 23Na NMR, *Biophys. J. 68* (3), 1063−1072.
26. Gross, L. M., and Strauss, U. P. (1966) in *Chemical Physics of Ionic Solutions* (Conway, B. E., Barradas, R. G., Eds.) pp 361−389, Wiley, New York.
27. Anderson, C. F., Record, M. T., Jr. (1980) The relationship between the Poisson-Boltzmann model and the condensation hypothesis: an analysis based on the low salt form of the donnan coefficient, *Biophys. Chem. 11*, 353−360.
28. Manning, G. S. (1969) Limiting Laws and Counterion Condensation in Polyelectrolyte Solutions I. Colligative Properties, *J. Chem. Phys. 51*, 924−933.
29. Anderson, C. F., and Record, M. T., Jr. (1983) in *Structure and Dynamics: Nucleic Acids and Proteins* (Clementi, E., Sarma, R., Eds.) pp 301−319, Adenine Press, New York.
30. Bloomfield, V. A., Crothers, D. M., and Tinoco, I., Jr. (2000) *Nucleic Acids: Structures, Properties, and Functions*, Chapter 6, University Science Books, Sausalito, CA.
31. Cohen, G., and Eisenberg, H. (1968) Deoxyribonucleate solutions: sedimentation in a density gradient, partial specific volumes, density and refractive index increments, and preferential interactions, *Biopolymers 6*, 1077−1100.
32. Zipper, P., and Bünemann, H. (1975) The interaction of actinomycin C3 and actinomine with DNA. A small-angle X-ray scattering study, *Eur. J. Biochem. 51*, 3−17.
33. Chapman, R. E., Jr., and Sturtevant, J. M. (1969) Volume changes accompanying the thermal denaturation of deoxyribonucleic acid. I. Denaturation at neutral pH, *Biopolymers 7*, 527−537.
34. Hearst, J. E. (1962) The specific volume of various cationic forms of deoxyribonucleic acid, *J. Mol. Biol. 4*, 415−417.
35. Durchschlag, H. (1986) in *Thermodynamic Data for Biochemistry and Biotechnology* (Hinz, H.-J., Ed.) p 72, Springer-Verlag, Berlin.
36. Arakawa, T., and Timasheff, S. N. (1983) Preferential interactions of proteins with solvent components in aqueous amino acid solutions, *Arch. Biochem. Biophys. 224*, 169−177.
37. Hamilton, D., and Stokes, R. H. (1972) Apparent molecular volumes of urea in several solvents as functions of temperature and concentration, *J. Solution Chem. 1*, 213−221.
38. Lo Surdo, A., Shin, C., and Millero, F. J. (1978) The apparent molal volume and adiabiatic compressibility of some organic solutes in water at 25 °C, *Chem. Eng. Data 23*, 197−201.
39. Archer, D. G. (1992) Thermodynamic properties of the NaCl + H_2O system II. Thermodynamic properties of NaCl(aq), NaCl·$2H_2O$(cr), and phase equilibria, *J. Phys. Chem. Ref. Data 21*, 793−829.
40. Archer, D. G. (1999) Thermodynamic properties of the KCl + H_2O system, *J. Phys. Chem. Ref. Data 28*, 1−17.
41. Smith, P. K., and Smith, E. R. B. (1940) Thermodynamic properties of solutions of amino acids and related substances. V. The activities of some hydroxy- and *N*-methylamino acids and proline in aqueous solution at twenty-five degrees, *J. Biol. Chem. 132*, 57−64.
42. Scatchard, G., Hamer, W. J., and Wood, S. E. (1938) Isotonic solutions. I. The chemical potential of water in aqueous solutions of sodium chloride, potassium chloride, sulfuric acid, sucrose, urea, and glycerol at 25 °C, *J. Am. Chem. Soc. 60*, 3061−3070.
43. Bevington, P. R., and Robinson, D. K. (1992) *Data reduction and error analysis for the physical sciences*, McGraw-Hill Inc., New York.
44. Holbrook, J. A., Capp, M. W., Saecker, R. M., and Record, M. T., Jr. (1999) Enthalpy and heat capacity changes for formation of an oligomeric DNA duplex: interpretation in terms of coupled processes of formation and association of single-stranded helices, *Biochemistry 38* (26), 8409−8422.
45. Richmond, T. J. (1984) Solvent accessible surface area and excluded volume in proteins. Analytical equations for overlapping spheres and implications for the hydrophobic effect, *J. Mol. Biol. 178*, 63−89.
46. Schneider, B., Patel, K., and Berman, H. M. (1998) Hydration of the phosphate group in double-helical DNA, *Biophys. J. 75*, 2422−2434.
47. Chalikian, T. V., Sarvazyan, A. P., and Breslauer, K. J. (1994) Hydration and partial compressibility of biological compounds, *Biophys. Chem. 51* (2−3), 89−107.
48. Schellman, J. A. (1990) A simple model for solvation in mixed solvents. Applications to the stabilization and destabilization of macromolecular structures, *Biophys. Chem. 37* (1−3), 121−140.
49. Schellman, J. A. (2003) Protein stability in mixed solvents: a balance of contact interaction and excluded volume, *Biophys. J. 85* (1), 108−125.
50. Anderson, C. F., Courtenay, E. S., and Record, M. T., Jr. (2002) Thermodynamic Expressions Relating Different Types of Preferential Interaction Coefficients in Solutions Containing Two Solute Components, *J. Phys. Chem. B 106*, 418−433.

51. Schreiner, L. J., Pintar, M. M., Dianoux, A. J., Volino, F., and Rupprecht, A. (1988) Hydration of NaDNA by neutron quasi-elastic scattering, *Biophys. J. 53* (1), 119−122.
52. Anderson, C. F., Felitsky, D., Hong, J., and Record, M. T., Jr. (2002) Generalized derivation of an exact relationship linking different coefficients that characterize thermodynamic effects of preferential interactions, *Biophys. Chem. 101*, 493−507.
53. Chalikian, T. V., Sarvazyan, A. P., Plum, G. E., and Breslauer, K. J. (1994) Influence of base composition, base sequence, and duplex structure on DNA hydration: apparent molar volumes and apparent molar adiabatic compressibilities of synthetic and natural DNA duplexes at 25 °C, *Biochemistry 33* (9), 2394−2401.
54. Gill, S. J., Dec, S. F., Olofsson, G., and Wadsoe, I. (1985) Anomalous heat capacity of hydrophobic solvation, *J. Phys. Chem. 89* (17), 3758−3761.
55. Fried, M. G., Stickle, D. F., Smirnakis, K. V., Adams, C., MacDonald, D., and Lu, P. (2002) Role of hydration in the binding of lac repressor to DNA, *J. Biol. Chem. 277* (52), 50676−50682.
56. Krakauer, H., and Sturtevant, J. M. (1968) Heats of the helix-coil transitions of the poly A-poly U complexes, *Biopolymers 6* (4), 491−512.
57. Privalov, P. L., Ptitsyn, O. B., and Birshtein, T. M. (1969) Determination of stability of the DNA double helix in an aqueous medium, *Biopolymers 8*, 559−571.
58. Record, M. T., Jr., Anderson, C. F., and Lohman, T. M. (1978) Thermodynamic analysis of ion effects on the binding and conformational equilibria of proteins and nucleic acids: the roles of ion association or release, screening, and ion effects on water activity, *Q. Rev.Biophys. 11* (2), 103−178.
59. Barone, G., Vecchio, P., D., Esposito, D., Fessas, D., and Graziano, G. (1996) Effect of osmoregulatory solutes on the thermal stability of calf-thymus DNA, *J. Chem. Soc., Faraday Trans. 92*, 1361−1367.
60. Robinson, D. R., and Jencks, W. P. (1965) The effect of compounds of the urea-guanidinium class on the activity coefficient of acetyltetraglycine ethyl ester and related compounds, *J. Am. Chem. Soc. 87*, 2462−2470.
61. Nandi, P. K., and Robinson, D. R. (1984) Effects of urea and guanidine hydrochloride on peptide and nonpolar groups, *Biochemistry 23*, 6661−6668.
62. Wang, A., and Bolen, D. W. (1997) A naturally occurring protective system in urea-rich cells: mechanism of osmolyte protection of proteins against urea denaturation, *Biochemistry 36*, 9101−9108.
63. Wetlaufer, D. B., Malik, S. K., Stoller, L., and Coffin, R. L. (1964) Nonpolar Group Participation in the Denaturation of Proteins by Urea and Guanidinium Salts. Model Compound Studies, *J. Am. Chem. Soc. 86*, 508−514.
64. Nozaki, Y., and Tanford, C. (1963) The solubility of amino acids and related compounds in aqueous urea solutions, *J. Biol. Chem. 238*, 4074−4081.
65. Zou, Q., Habermann-Rottinghaus, S. M., and Murphy, K. P. (1998) Urea effects on protein stability: hydrogen bonding and the hydrophobic effect, *Proteins 31*, 107−115.
66. Felitsky, D. J., Cannon, J. G., Capp, M. W. Hong, J., VanWynsberghe, A. W., Anderson, C. F., and Record, M. T., Jr. (2004) The Exclusion of Glycine Betaine from Anionic Biopolymer Surface: Why Glycine Betaine Is an Effective Osmoprotectant but Also a Compatible Solute, *Biochemistry 43*, 14732−14743..
67. Felitsky, D. J., and Record, M. T., Jr. (2004) Application of the local−bulk partitioning and competitive binding models to interpret preferential interactions of glycine betaine and urea with protein surface, *Biochemistry 43* (28) 9276−9288.
68. Shelton, V. M., Sosnick, T. R., and Pan, T. (1999) Applicability of urea in the thermodynamic analysis of secondary and tertiary RNA folding. *Biochemistry 38*, 16831−16839.

BI049096Q